AD-A034 420   AIR FORCE GEOPHYSICS LAB HANSCOM AFB MASS   F/G 4/1
               A HIGH-LATITUDE EMPIRICAL MODEL OF SCINTILLATION EXCURSIONS: PH--ETC(U)
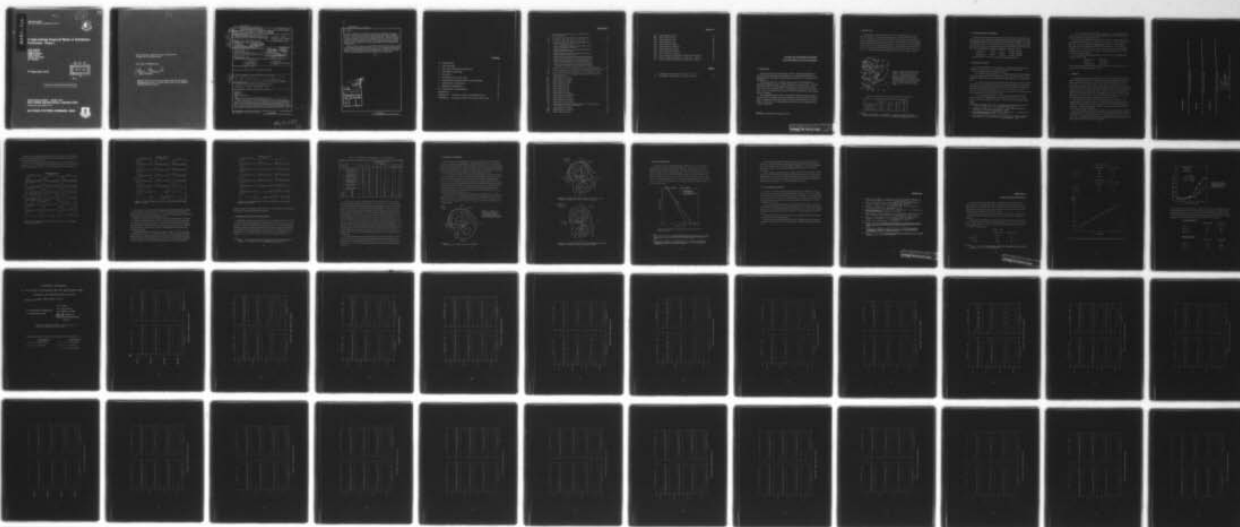   SEP 76   J AARONS, J MULLEN, H WHITNEY
UNCLASSIFIED   AFGL-TR-76-0210   NL
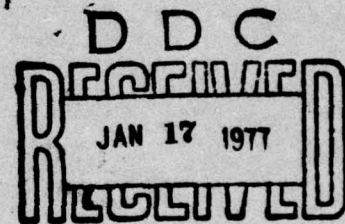
| OF |
AD
A034420

END

DATE
FILMED

2-77

AFGL-TR-76-0210
AIR FORCE SURVEYS IN GEOPHYSICS, NO. 353

A High-Latitude Empirical Model of Scintillation Excursions: Phase I

JULES AARONS
JOHN MULLEN
HERBERT WHITNEY
EILEEN MARTIN
KRISHIN BHAVNANI
LEO WHELAN

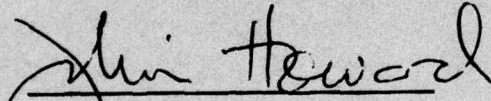17 September 1976

D D C
RECEIVED
JAN 17 1977
A

SPACE PHYSICS DIVISION   PROJECT 4643
AIR FORCE GEOPHYSICS LABORATORY
HANSCOM AFB, MASSACHUSETTS 01731

AIR FORCE SYSTEMS COMMAND, USAF

This technical report has been reviewed and
is approved for publication.

FOR THE COMMANDER:

Chief Scientist

REPORT DOCUMENTATION PAGE	READ INSTRUCTIONS BEFORE COMPLETING FORM

1. REPORT NUMBER	2. GOVT ACCESSION NO.	3. RECIPIENT'S CATALOG NUMBER
AFGL-TR-76-0210	AFGL-AFSG-353	

4. TITLE (and Subtitle)	5. TYPE OF REPORT & PERIOD COVERED
A HIGH-LATITUDE EMPIRICAL MODEL OF SCINTILLATION EXCURSIONS: PHASE I	Scientific. Interim.
	6. PERFORMING ORG. REPORT NUMBER
	AFSG No. 353

7. AUTHOR(s)	8. CONTRACT OR GRANT NUMBER(s)
Jules Aarons, Eileen Martin* John Mullen, Krishin Bhavnani** Herbert Whitney, Leo Whelan**	

9. PERFORMING ORGANIZATION NAME AND ADDRESS	10. PROGRAM ELEMENT, PROJECT, TASK AREA & WORK UNIT NUMBERS
Air Force Geophysics Laboratory (PHP) Hanscom AFB, Massachusetts 01731	62101F 46430104 01

11. CONTROLLING OFFICE NAME AND ADDRESS	12. REPORT DATE
Air Force Geophysics Laboratory (PHP) Hanscom AFB, Massachusetts 01731	17 September 1976
	13. NUMBER OF PAGES
	58

14. MONITORING AGENCY NAME & ADDRESS(if different from Controlling Office)	15. SECURITY CLASS. (of this report)
56p.	Unclassified
	15a. DECLASSIFICATION/DOWNGRADING SCHEDULE

16. DISTRIBUTION STATEMENT (of this Report)

Approved for public release; distribution unlimited.

17. DISTRIBUTION STATEMENT (of the abstract entered in Block 20, if different from Report)

Air Force surveys in geophysics

18. SUPPLEMENTARY NOTES

*Emmanuel College, Boston, Massachusetts 02115

**Logicon Inc., Bedford, Massachusetts 01730

19. KEY WORDS (Continue on reverse side if necessary and identify by block number)

Scintillation
Auroral
High latitude model

20. ABSTRACT (Continue on reverse side if necessary and identify by block number)

Using observations of the scintillations of beacons from synchronous satellites, a high latitude model of scintillation excursion is being developed. Phase 1 of the development has been completed and is described in this report. Several years of continuous recordings taken at Narssarssuaq, Greenland, Goose Bay, Labrador, and Sagamore Hill, Massachusetts, were reduced. The data base consists of values of 15-min scintillation excursions in dB at

next page

DD FORM 1473 EDITION OF 1 NOV 65 IS OBSOLETE
1 JAN 73

409578 LB

Cont

20. (Cont)

137 MHz. Equations are developed which yield scintillations at this frequency as a function of local time, magnetic index, solar flux, and month of the year. The concept is to predict, at sub-auroral and auroral latitudes, scintillation at this frequency and at higher frequencies. The aim is to give to users an indication of expected scintillation excursion when one predicts magnetic activity and solar radio flux. The equations developed have been checked with one additional set of observations and are being checked with additional data.

Phase 2 of this model will incorporate geometrical terms to take account of the propagation angle of the observer vis-a-vis the irregularities and will allow for frequency dependence to be ascertained. In addition, it is expected in Phase 2 to validate the model with additional sets of data, extending the model to auroral latitudes greater than 63° and to polar latitudes.

deg

White Section
Buff Section
UNANNOUNCED
JUSTIFICATION.............................

BY..
DISTRIBUTION/AVAILABILITY CODES
Dist.   AVAIL. and/or SPECIAL

Contents

3

Illustrations

Tables

A High-Latitude Empirical Model
of Scintillation Excursions: Phase 1

1. INTRODUCTION

In order to provide a realistic series of values to determine scintillation occurrence at sub-auroral and auroral latitudes, the Trans-Ionospheric Branch of the Space Physics Laboratory in collaboration with Logicon, Inc. initiated a model development.

The data base was to be a series of measurements of the scintillations of synchronous satellite beacons at 137 MHz extending over several years. The initial model was to provide mean scintillation excursions as a function of time of day, month, solar flux, and magnetic index. With forecasting of solar flux and magnetic index, a user in the latitude range covered would have an indication of mean scintillations to be expected.

The information would be useful in estimating scintillations at higher frequencies such as 250 to 400 MHz and at other geometries in the sub-auroral and auroral ovals. In addition the data could be used to forecast clutter problems on HF backscatter systems that show difficulties from the same F layer irregularities that produce scintillations.

2. THE DATA BASE

Observations of the scintillations of the ATS-3 satellite beacon at 137 MHz form the data base. The data was reduced by the method outlined by Whitney et al.[1] Scintillation excursions in dB for 15-min periods are used; these approximately correspond to the 1% percentile levels in the cumulative amplitude probability distribution function for the 15-min period. The dB excursions are convertible into S_4 indices by an empirical relationship. The three stations are situated near the 70° West meridian, and their propagation paths to the ATS-3 satellite are shown in Figure 1. Their geomagnetic and geometrical parameters are given in Table 1.
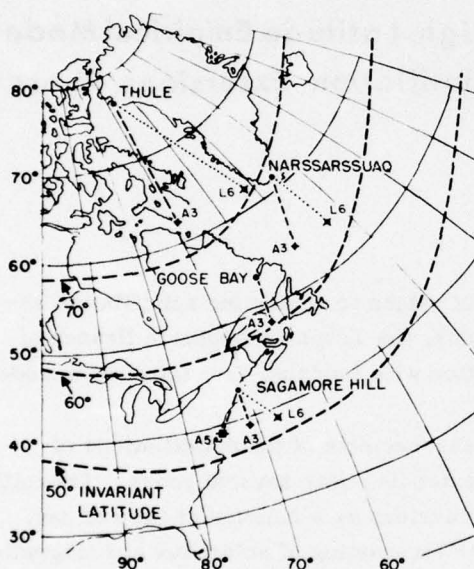
Figure 1. Observing Stations (ATS-3 at 70°W, LES-6 at 39°W, ATS-5 at 105°W). Thule data was not used in Phase 1. X denotes the 350 km intersection point to the satellite. Propagation paths to ATS-3 are shown as well as those to LES-6 and ATS-5. Only data from ATS-3 was used in Phase 1. Other data will be used in Phase 2

Table 1. Geomagnetic and Geometrical Parameters for ATS-3

	Inv. Lat.	El.	Az.	Iono. Z.A.
Narssarssuaq	63.2°	18.0°	208°	64°
Goose Bay	60.3°	28.8°	191°	56°
Sagamore Hill	53.5°	40.9°	178°	46°

1. Whitney, H.E., Malik, C., and Aarons, J. (1969) A proposed index for measuring ionospheric scintillations, Planet. Space Science, 17:1069-1073.

3. DATA BASE CREATION AND MODELING

Fifteen-minute samples of scintillation index (dB) data for the ATS-3 satellite from the above three stations have been augmented into complete data bases on tape. Data associated with each 15-min sample include: Station ID, Satellite ID, Frequency (137 MHz), Date and UT, Scintillation Index (dB), 3-hourly magnetic index (K_p), 2695 MHz solar flux, (S_f), 4995 MHz solar flux, sub-ionospheric latitude and longitude, and corresponding geomagnetic latitude and magnetic local time.

Narssarssuaq	9/17/68 - 9/1/74	146,700 + samples
Goose Bay	1/1/72 - 12/31/74	71,000 + samples
Sagamore Hill	12/1/69 - 11/30/74	148,000 + samples

Goose Bay data for 1974 cover mainly November and December.

4. THE FORCING FUNCTIONS

In the initial development, termed Phase 1, a relatively simple equation was developed to reproduce the mean scintillation excursions at each station.

The forcing parameters included the following:

(a) Planetary magnetic index, K_p. It has been shown that at high latitudes (which in this case include the Narssarssuaq and Goose Bay observations and, during severe magnetic storms, the Sagamore Hill observations) K_p is a forcing function.[2]

(b) Early work by Aarons et al[3] showed that solar flux, even when divorced from magnetic index variations, had an effect on scintillation behavior. Utilizing the 2695 MHz solar measurements at Sagamore Hill,[4] we separated observations into three regimes of solar flux units (S_f); (1) 0-95, (2) 96-120, and (3) 121 and greater. As will be shown scintillations do not in every month increase with increasing solar flux but vary as a function of season.

(c) The seasonal parameter. A very dramatic minimizing of diurnal effects is shown in the Narssarssuaq observations over the winter.[5] A similar pattern is seen on the Goose Bay records. This would have to be reflected in the model.

2. Aarons, J. and Allen, R.S. (1971) Scintillation boundaries during quiet and disturbed magnetic conditions, J. Geophys. Res., 76:170-177.

3. Aarons, J., Whitney, H.E., and Allen, R.S. (1971) Global morphology of ionospheric scintillations, Proc. IEEE., 59:159.

4. Solar-Geophysical Data, IER-FB 289-304, 305-364 Part I, U.S. Department of Commerce (Boulder, Colorado, U.S.A. 80302).

5. Basu, Sunanda (1975) Universal time seasonal variations of auroral zone magnetic activity and VHF scintillations, J. Geophys. Res., 80:4725-4728.

(d) The diurnal pattern would have to be shown. This would include the variations as a function of local time under magnetically quiet and disturbed conditions as modulated by the seasonal function.

Analyses were conducted separately for each station. The data were further partitioned into 12 months, 7 K_p, 3 Solar Flux (2.7 GHz), and 24 UT ranges. The date, K_p, S_f and SI readings were <u>averaged</u> in each block. A compact file was thus made available for high speed iterative modeling studies. The seven K_p ranges are 0-1, 1+ to 2, 2+ to 3, 3+ to 4, 4+ to 5, 5+ to 6, 6+ and up. The three S_f ranges are 0 to 95, 96 to 120, 121 and up. Tables of the averaged SI are provided for each of the stations.

Out of a maximum possible 6048 blocks (12 x 7 x 3 x 24), the averaged files comprise the following:

Narssarssuaq	4985 blocks
Goose Bay	4217 blocks
Sagamore Hill	5065 blocks.

The empty blocks generally correspond to the highest two K_p ranges, that is, 5+ and up, and occasionally the highest S_f range.

5. MODELING

An extensive search was conducted to derive empirical models of SI for each of the three stations (Figure 2a). Analytical forms of the model were preferred to ensure smooth transitions as a function of the known driving functions, namely, day of year, K_p, S_f and universal time. These forms also permitted use of regression techniques for least squares fitting to the averaged data file. In the course of the search for improved fits, special characteristics of the data were noted which suggested elaborations of the model form. Examples are the delayed peak in the diurnal SI variation with higher K_p, the seasonal effect on diurnal variation amplitude relative to the average SI, the seasonal effect on influence of K_p and S_f, and the need for higher harmonics to represent the diurnal variation.

The models for average SI (dB) for the three stations are provided. In the model equations, the cosine arguments (in radians) that include the terms for day number (DA) and hour (HR) assume a multiplicative term of $2\pi/365$ and $2\pi/24$ respectively. Though not shown in the equation for reasons of convenience, these must be included in the calculations.

Figure 2b presents the model for each station in terms of local time. The difference between universal time and local time at the sub-ionospheric point (350 km) was taken to be 3.4 hr at Narssarssuaq, 4.1 hr at Goose Bay, and 4.7 hr at Sagamore Hill. Subsequent work directed towards developing bridging models used local time rather than universal time as the argument.

10

NARSSARSSUAQ

$$SI(dB) = -6.4 + 9.2(1-.2FD)\left[1+.23(1-.3FD)\cos(HR-1.4-.34Kp)+.03\cos(2(HR-4.0))+.02\cos(3(HR-4))\right]2^{\left[.14Kp(1+.12FD)+.09As(1+1.76FD)\right]}$$

$$FD = \cos(DA+15.6) + .56\cos(2(DA-22.4))$$

GOOSE BAY

$$SI(dB) = -1.3 + 1.1(1-.77FD)\left[1+.5(1-.2FD)\cos(HR-2.0-.6Kp)+.06\cos(2(HR-6.2))+.02\cos(3(HR+1.1))\right]2^{\left[.3Kp(1+.1FD)+.8As(1+1.2FD)\right]}$$

$$FD = \cos(DA+.5) + .2\cos(2(DA-99))$$

SAGAMORE HILL

$$SI(dB) = 0.33 + .02(1+.2FD)\left[1+1.2(1-.01FD)\cos(HR-5.1-.15Kp)+.3\cos(2(HR-5.5))-.1\cos(3(HR+1.4))\right]2^{\left[.38Kp(1+.3FD)+3.1As(1-.2FD)\right]}$$

$$FD = \cos(DA+56) + .7\cos(2(DA-143))$$

DA – DAY NUMBER
As = S_f/100
S_f – SOLAR FLUX AT 2695 MHz
   IN SOLAR FLUX UNITS

HR IS UNIVERSAL TIME

Figure 2a. Scintillation Index (dB) Models for Universal Time

11

NARSSARSSUAQ

$$SI(dB) = -6.4 + 9.2(1-.2FD)\left[1+.23(1-.3FD)\cos(HL+2.0+.34Kp)+.03\cos(2(HL-0.6)+.02\cos(3(HL+3.0))\right]2^{\left[.14Kp(1+.12FD)\, +\, .09As(1+1.76FD)\right]}$$

$$FD = \cos(DA+15.6) + .56\cos(2(DA-22.4))$$

GOOSE BAY

$$SI(dB) = -1.3 + 1.1(1-.77FD)\left[1+.5(1-.2FD)\cos(HL+2.1-.6Kp)+.06\cos(2(HL-2.1))+.02\cos(3(HL+5.2))\right]2^{\left[.3Kp(1+.1FD)+.8As(1+1.2FD)\right]}$$

$$FD = \cos(DA+.5) + .2\cos(2(DA-99))$$

SAGAMORE HILL

$$SI(dB) = 0.33+.02(1+.2FD)\left[1+1.2(1-.01FD)\cos(HL-0.4-.15Kp) + .3\cos(2(HL-0.8))-.1\cos(3(HL+6.1))\right]2^{\left[.38Kp(1+.3FD)+3.1As(1-.2FD)\right]}$$

$$FD = \cos(DA+56) + .7\cos(2(DA-143))$$

DA – DAY NUMBER

As = S_f / 100

HL – LOCAL TIME (hours) AT SUB-IONOSPHERIC POINT (350 km)

S_f – SOLAR FLUX AT 2695 MHz IN SOLAR FLUX UNITS

Figure 2b. Scintillation Index (dB) Models for Local Time

12

In Figures 3 to 6 typical comprehensive comparative plots of the averaged data and the model are provided for each station. The model predictions used the actual averaged data, K_p and S_f for each hour, and are therefore absent when data are absent. These best fit models may occasionally predict small negative SI's; these are made to asymptotically approach zero by replacing a value V which is less than 0.5 by $e^{2(V-.85)}$. This ensures continuity in the predictions near 0.5 and introduces minimal distortion since only the very low scintillations are adjusted.

6. THE EQUATIONS AND THE DATA

To illustrate the behavior of the data and of the best fitting model equations, Narssarssuaq data is shown in Figure 3 for the month of March. One can note, for example, along the left-hand side for the solar flux set of 0 to 95, that scintillations increase with increasing K_p. The dotted line is the model equation and the continuous line connects 1-hr means of scintillation excursions.
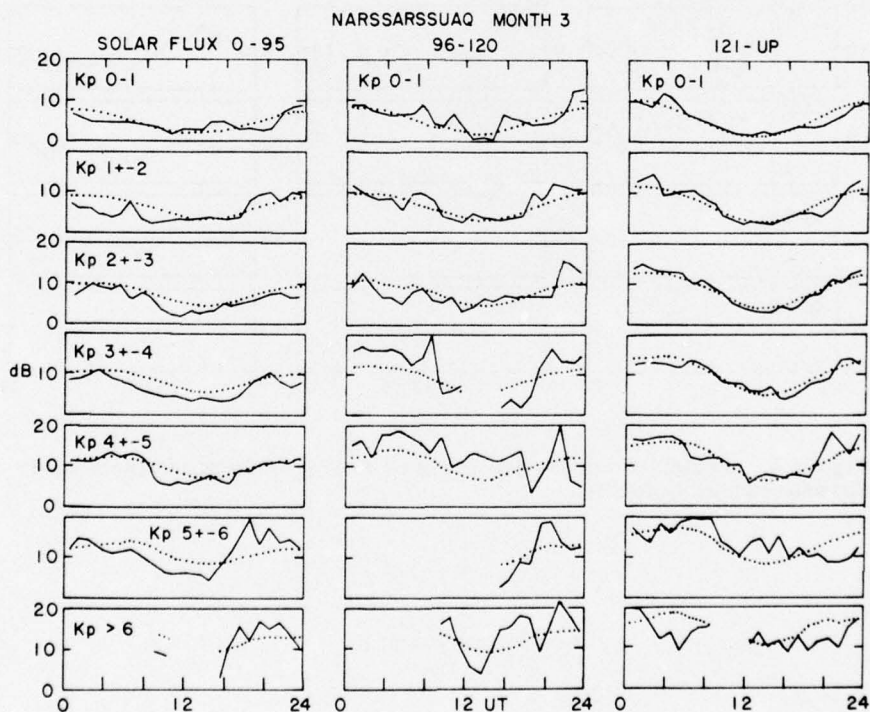
Figure 3. Typical Comparative Plots of Averaged Data and the Model; Narssarsuaq, March

13

Along any series of boxes with identical K_p one can note that the model and the data indicate that the general trend is for the scintillation excursions to increase with increasing solar flux.

In the Narssarssuaq data for October (Figure 4) it can be noted that with increasing K_p (for a constant solar flux) scintillation excursions increase, and the scintillation excursions decrease with increasing solar flux (and constant K_p).
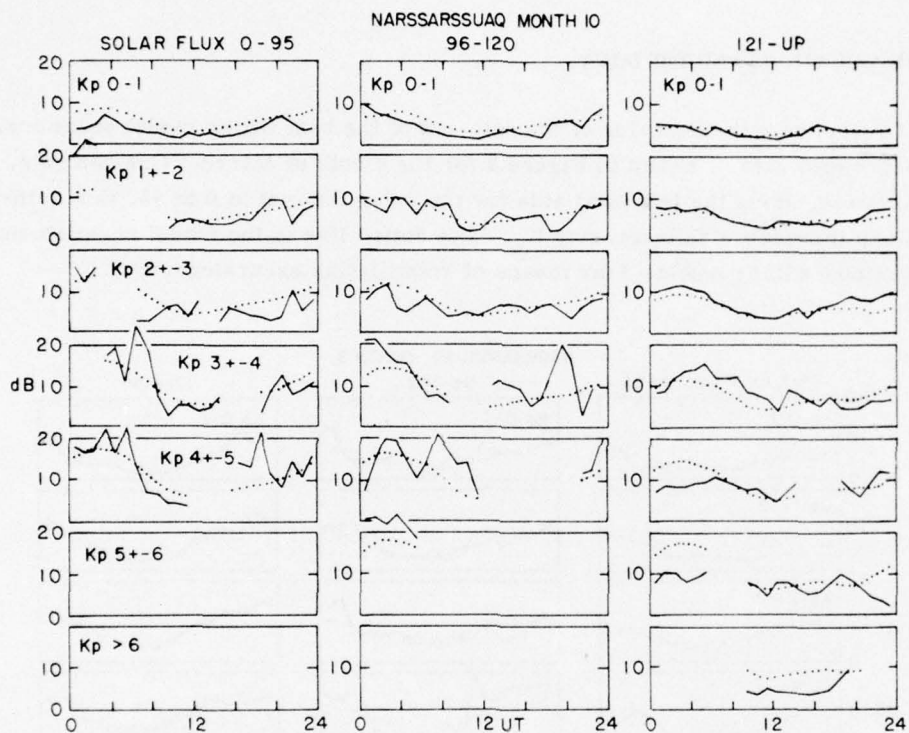

Figure 4. Typical Comparative Plots of Averaged Data and the Model; Narssarssuaq, October
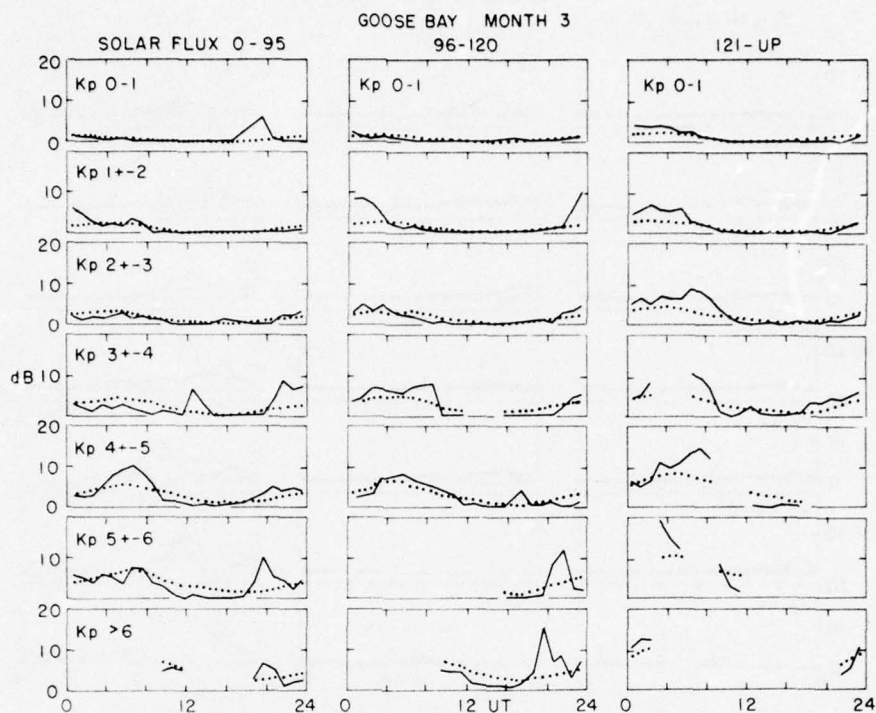
14

Figure 5. Typical Comparative Plots of Averaged Data and the Model; Goose Bay, March

The behavior of the Goose Bay data (solid line) and best-fitting model (dashed line) for March are shown in Figure 5. Within each particular solar grouping scintillations increase with increasing K_p. For the same K_p grouping, the scintillation excursions increase with increasing solar flux.

Behavior of the Sagamore Hill data and model for March are shown in Figure 6. For the low solar flux group (0 to 95), a very slight increase in scintillations associated with increasing K_p is seen. The same is true of the solar flux group 96 to 120 while for high solar flux, the increase with K_p becomes more noticeable. In general, within a particular K_p grouping, scintillation index increases with increasing solar flux.

Although equations were developed for Sagamore Hill, Goose Bay, and Narssarssuaq observations, it is not certain whether or not to join the Sagamore Hill observations to the high latitude data in the model which will be finally developed. The sub-auroral to middle latitudes traversed (at 53° invariant latitude) present a different morphology from the high latitude ionosphere except during periods of
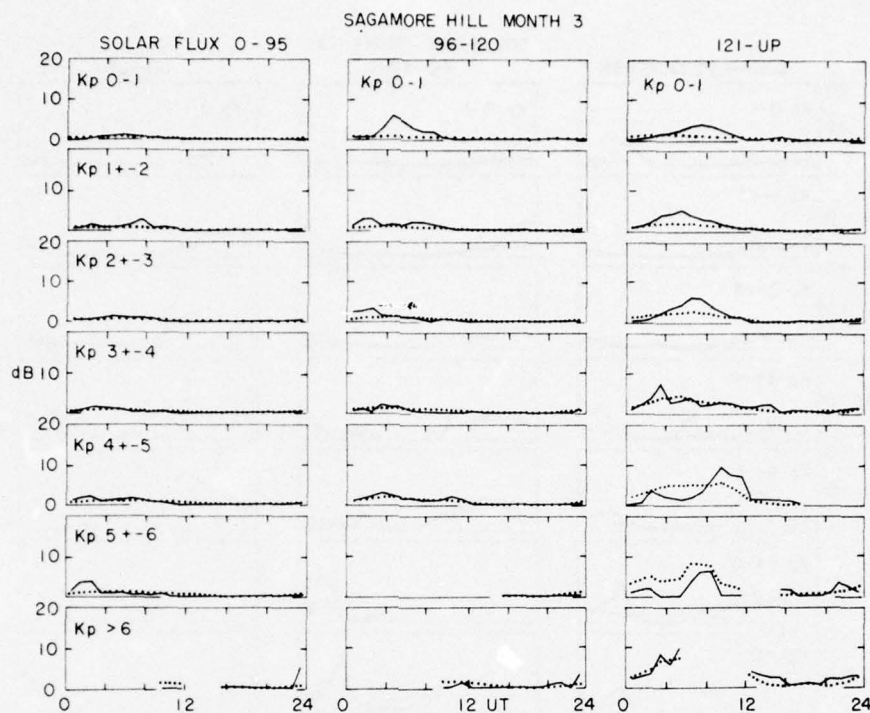
15

Figure 6. Typical Comparative Plots of Averaged Data and the Model; Sagamore Hill, March

intense magnetic activity when auroral effects at F layer heights cover this region. [6] Further work on this is exhibited in Appendix B.

7. DISTRIBUTION OF SCINTILLATION INDEX READINGS

Distribution analyses were conducted for each of the three stations. The effect of the solar flux was not evaluated, but partitioning by month, K_p, and hour was retained. Within each partition the average SI was calculated, and the percentage of readings falling in consecutive ranges was determined. Significant features of the distributions have been obtained by examination of the tabulations, and are discussed below. For selected average SI, the percentage SI readings found in the ranges 0-1, 1-3, 3-6, 6-9, 9-12, and 12 and up are presented in Table 2.

---

6. Aarons, J. (1976) High-latitude irregularities during the magnetic storm of October 31 to November 1, 1972, J. Geophys. Res., 81:661-670.

Table 2. Distribution of SI Readings for Various Average SI

Avg. SI		Percent Occurrence SI Range					
		0-1	1-3	3-6	6-9	9-12	12 up
1.0	Narssarssuaq	50	45	5	0	0	0
	Goose Bay	55	35	9	1	0	0
	Sagamore Hill	70	15	10	3	2	0
2.0	Narssarssuaq	20	55	20	4	1	0
	Goose Bay	40	40	15	3	1	1
	Sagamore Hill	55	25	10	5	3	2
3.0	Narssarssuaq	20	40	25	10	3	2
	Goose Bay	30	33	18	10	5	4
	Sagamore Hill	50	20	12	7	5	6
4.0	Narssarssuaq	10	38	28	15	4	5
	Goose Bay	20	33	20	15	5	7
5.0	Narssarssuaq	6	33	30	18	5	8
	Goose Bay	12	30	25	18	6	9
6.0	any	3	25	35	20	6	11
8.0	any	2	15	25	20	16	22
10.0	any	1	6	15	18	20	40
13.0	any	1	1	8	10	20	60

For each station, no marked variations in the distributions are evident for different months, K_p ranges or time of day. Thus, given an average SI value for any time-K_p partition for a specific station, the expectation of any range of readings may be predicted. Differences in distribution patterns among the three stations are primarily due to the consistently higher SI readings at Narssarssuaq on the one hand, and the extremely low activity at Sagamore Hill on the other; 0 to 1 dB readings are rarer at Narssarssuaq so that average SI of 1 to 3 dB are found with negligible occurrence at the higher SI readings. At Sagamore Hill 0 to 1 dB readings constitute more than 50 percent of the samples at any time so that an average of even 1 dB implies the presence of some high SI readings. Though the 1 to 3 dB averages usually occur in the daytime at Narssarssuaq and in the night sector at Sagamore Hill, no particular diurnal influence is evident on the distributions. Thus, the instances where low average SI are found in the nighttime at Narssarssuaq are devoid of higher SI readings as in the daytime; the instances where average SI at Sagamore Hill are over 1 dB in the daytime, higher sporadic SI readings are clearly the cause.

The above discussion covers the latitudinal and SI activity extremes. Goose Bay lies in between and characteristics consistent with the above arguments are exhibited in the distributions for this station. As seen in Table 2, below an average of 6 dB, Goose Bay readings tend to include more high SI samples than Narssarssuaq.

17

8. GEOMETRICAL PARAMETERS

The development of the equations in the form given fails to correct scintillations for the geometry of observations. Scintillations maximize at low angles of elevation and when the signal is observed parallel to the lines of force of the earth's field. The complexity of arriving at a physical model which determines the elongation of the irregularities as a function of latitude, time, and geomagnetic conditions is such that only a simplified solution can be attempted at this time.

In a preliminary attempt to give to the user of this Phase 1 model a correction factor for geometry we have, from studies at Narssarssuaq, Goose Bay, and Sagamore Hill[7] presented an elliptical column model of individual irregularities of 1 km N-S, 2 km orthogonal to the lines of force and 5 km along the lines of force. Assuming a Gaussian irregularity spectrum, it was determined that the correction for the S_4 value derived from each index would be a factor of ~2.0 greater at the azimuth and elevation of the ATS-3 satellite from Narssarssuaq than at zenith. From Goose Bay the correction factor using the same model would be ~1.3, and from Sagamore Hill it would be ~1.4.

Graphs of these correction factors have been developed, these are given in Figures 7, 8, and 9. It should be noted that the model equations have not utilized these correction factors; the factors are given merely to help the reader. It is expected that in Phase 2 of the model development a geometrical correction factor will be utilized.
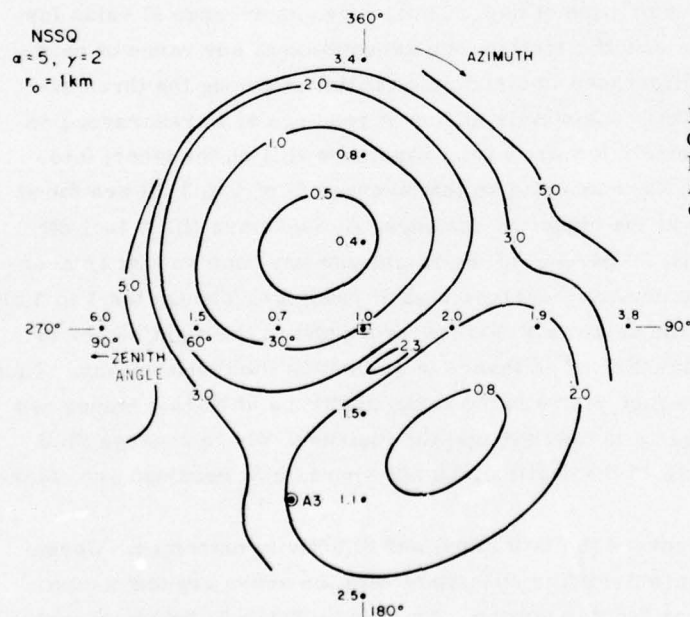

Figure 7. Graph of Correction Factors for Narssarssuaq Under Assumptions of Elliptical Column Irregularity Model

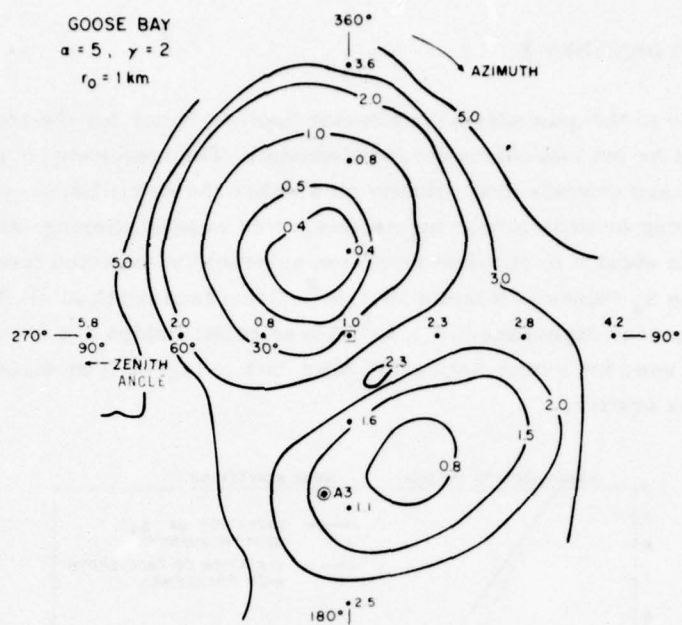7. Singleton, D. G. (1975) Private communication.

18

GOOSE BAY
$a = 5$, $\gamma = 2$
$r_0 = 1$ km

360°
AZIMUTH

270° — 90°
ZENITH ANGLE

180°

Figure 8.   Graph of Correction Factors for Goose Bay Under
Assumption of Elliptical Column Irregularity Model

SAGAMORE HILL
$a = 5$ $\gamma = 2$
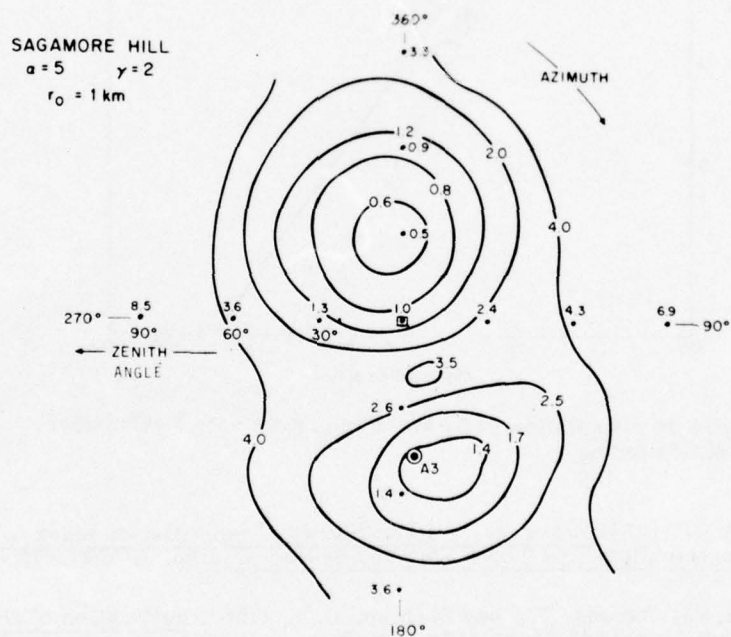$r_0 = 1$ km

360°
AZIMUTH

270° — 90°
ZENITH ANGLE

180°

Figure 9.   Graph of Correction Factors for Sagamore Hill Under
Assumption of Elliptical Column Irregularity Model

19

9. FREQUENCY DEPENDENCE

In addition to the geometrical parameter another factor for the frequency dependence must be put into the model development. The frequency correction is quite complex and depends dramatically on whether the scintillations are in the strong scattering or weak scattering regime. For weak scattering (with dB excursions less than about 8 in our data reduction scheme) the expected frequency dependence using S_4 values is a factor of 1.5.[8] Using fade depth in dB (below mean level) the frequency dependence is 1.9.[9] These relationships are shown in Figure 10 and can be used for extrapolating 137 MHz data to higher frequencies under conditions of weak scatter.
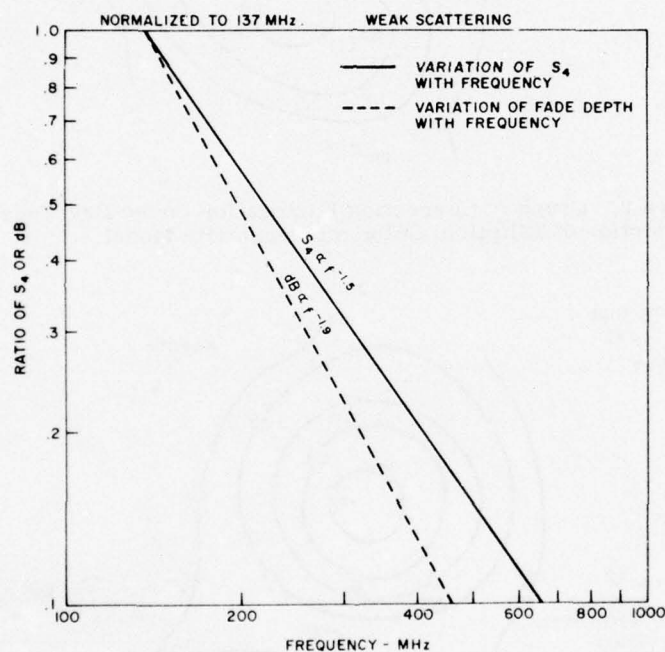
Figure 10. Variation of S_4 and Fade Depth with Frequency; Weak Scattering

8. Whitney, H.E. (1974) Notes on the Relationship of Scintillation Index to Probability Distributions and Their Uses for System Design, AFCRL-TR-74-0004.

9. Whitney, H.E., Aarons, J., and Seeman, D.R. (1971) Estimation of the Cumulative Amplitude Probability Distribution Function of Ionospheric Scintillations, Appendix I, AFCRL-71-0525.

With strong scattering the frequency dependence term for S_4 will vary from zero to 1.5. The zero frequency dependence occurs when reduced simultaneous data at two frequencies both display Rayleigh distributions. Frequency dependence then may vary from zero to the weak scattering regime value of 1.9 based on fade depth.

With a frequency dependence term, a proper model for the irregularity configuration, and a geophysically valid model of the effect of the polar cap, auroral and sub-auroral terms, it will be possible to further develop this model so that it can service systems designers and operators who have radio transmissions affected by high latitude irregularities. This will be attempted in Phase 2.

10. FUTURE MODEL DEVELOPMENT

Phase 2 of the model development will incorporate in its equations, corrections for geometry utilizing newly developed data on power law fall off of irregularity spectra as a function of latitude and geomagnetic conditions. An attempt will be made to utilize the data set out in this development by dividing the observations into weak and strong scatter regimes to determine frequency dependence for various scintillation excursions.

Phase 2 also envisages additional validation studies of the model. Data from new satellites will be used to check the observations in the auroral and sub-auroral regions and to extend the observations into the polar area. The Goose Bay data base was considerably smaller than the other stations'; it will be expanded for the final model.

The use of satellites at low and high altitudes transmitting at several frequencies will allow for high latitude studies.

Multi-frequency transmissions will also allow additional studies of frequency dependence to determine how best to extend these 137 MHz data to higher frequencies.

21

References

1. Whitney, H. E., Malik, C., and Aarons, J. (1969) A proposed index for measuring ionospheric scintillations, Planet. Space Science, 17:1069-1073.

2. Aarons, J. and Allen, R. S. (1971) Scintillation boundaries during quiet and disturbed magnetic conditions, J. Geophys. Res., 76:170-177.

3. Aarons, J., Whitney, H. E., and Allen, R. S. (1971) Global morphology of ionospheric scintillations, Proc. IEEE., 59:159.

4. Solar-Geophysical Data, IER-FB 289-304, 305-364 Part I, U.S. Department of Commerce (Boulder, Colorado, U.S.A. 80302).

5. Basu, Sunanda (1975) Universal time seasonal variations of auroral zone magnetic activity and VHF scintillations, J. Geophys. Res., 80:4725-4728.

6. Aarons, J. (1976) High-latitude irregularities during the magnetic storm of October 31 to November 1, 1972, J. Geophys. Res., 81:661-670.

7. Singleton, D. G. (1975) Private communication.

8. Whitney, H. E. (1974) Notes on the Relationship of Scintillation Index to Probability Distributions and Their Uses for System Design, AFCRL-TR-74-0004.

9. Whitney, H. E., Aarons, J., and Seeman, D. R. (1971) Estimation of the Cumulative Amplitude Probability Distribution Function of Ionospheric Scintillations, Appendix I, AFCRL-71-0525.

10. Evans, J. V., ed. (1973) The Millstone Hill Radar Propagation Study: Scientific Results, Lincoln Lab. Technical Report.

Appendix A

Comparison of Model With Millstone Hill Data

In order to validate the model using an independent set of observations at a higher frequency it was determined that the Millstone Hill data obtained by observing scintillations at 400 MHz tracking Transit satellites would be used. The data base for the comparison was that in the publication "The Millstone Hill Radar Propagation Study: Scientific Results"[10] by J. Evans.

Since Evans' data was in the S_4 format at 400 MHz, a conversion using weak scatter relationships must first be made to dB at 137 MHz. This is plotted in Figure A1.

The measured S_4 (400 MHz) as a function of invariant latitude is shown in Figure A2. These values, in three different K_p groupings, at the invariant latitude of Narssarssuaq, Goose Bay, and Sagamore Hill, along with the conversion to dB (137 MHz)[9] is shown below.

	NSSQ ($\Lambda = 63°$)	
	S_4 (400 MHz)	dB (137 MHz)
$K_p \leq 1+$	.0375	2.5
$2_o \leq K_p \leq 3+$	.05	3.6
$K_p \geq 4_o$	.0760	6.2

---

10. Evans, J. V., ed. (1973) The Millstone Hill Radar Propagation Study: Scientific Results, Lincoln Lab. Technical Report.

Goose Bay ($\Lambda = 60°$)

	S_4 (400 MHz)	dB (137 MHz)
$K_p \leq 1+$	.025	1.5
$2_o \leq K_p \leq 3°$	.028	1.8
$K_p \geq 4_o$	.055	4.0

Sagamore Hill ($\Lambda = 54°$)

	S_4 (400 MHz)	dB (137 MHz)
$K_p \leq 1+$	.016	.8
$2_o \leq K_p \leq 3+$	.018	1.0
$K_p \geq 4_o$	.021	1.2
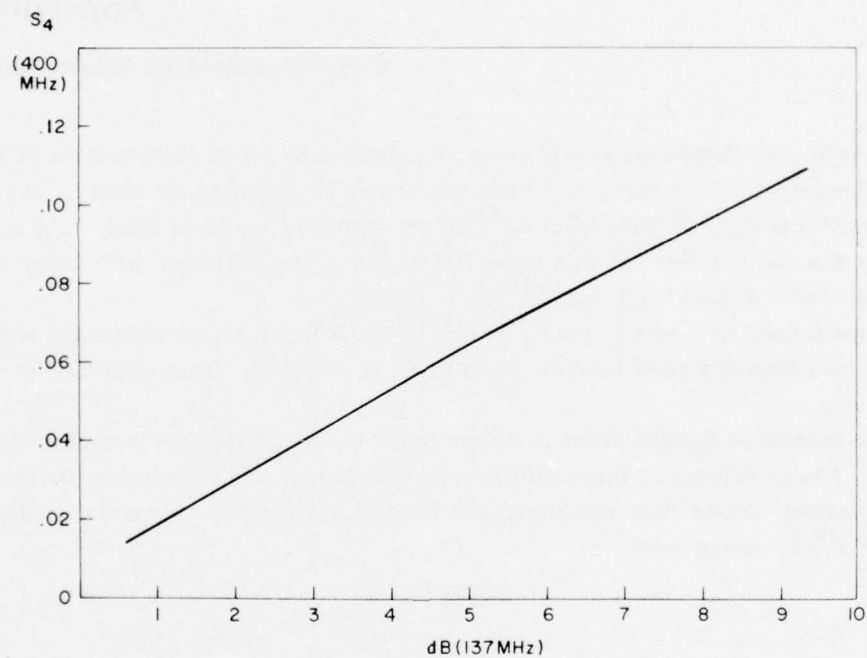
Figure A1. Relationship Between S_4 at 400 MHz and Scintillation (dB) at 137 MHz
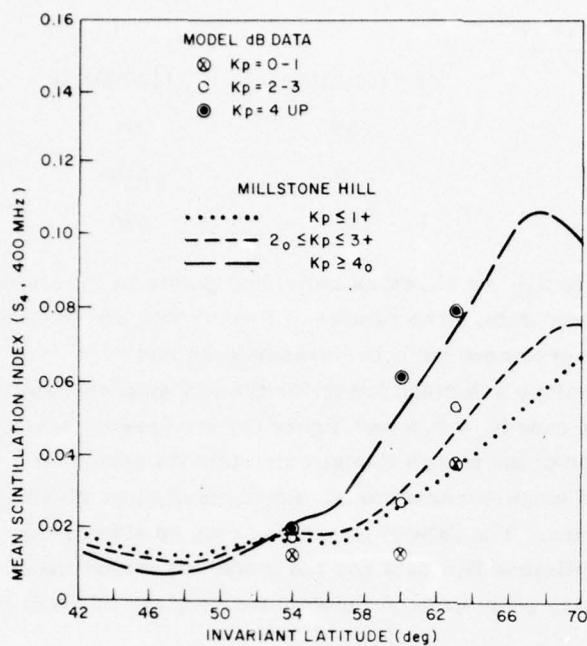
Figure A2. Mean Scintillation Index for Different Levels of Magnetic Activity

This data used by Evans was taken in 1972 and 1973, and was averaged over local time to include all passes. The model dB values are obtained by using the local time equations shown in Figure 2b for each station for three particular K_p values. A solar flux level of $S_f = 108$ was used since solar flux in 1972 and 1973 was of this magnitude. The resulting averages over all hours and all months are:

Narssarssuaq (63° Λ)

	dB (137 MHz)	S_4 (400 MHz)
K_p = .5	2.5	.0375
K_p = 2.5	4.0	.053
K_p = 5.0	6.3	.0775

Goose Bay (60° Λ)

	dB (137 MHz)	S_4 (400 MHz)
K_p = .5	.3	.012
K_p = 2.5	1.6	.026
K_p = 5.0	4.8	.063

27

Sagamore Hill (54° Λ)

	dB (137 MHz)	S_4 (400 MHz)
K_p = .5	.55	.014
K_p = 2.5	.75	.0155
K_p = 5.0	1.12	.020

The model dB values (converted to S_4) are shown as individual points in Figure A2 to facilitate comparison with Evans' data. The results of Evans' data and the model dB values predicted are in good agreement for both Narssarssuaq and Sagamore Hill. At Goose Bay, the model values are much lower for the low magnetic activity case, somewhat lower for the case K_p = 2.5 and higher for the case K_p = 5.0.

It is believed that the position of the trough is approximately the invariant latitude of Goose Bay under quiet magnetic conditions, moving farther south as the level of magnetic activity increases. The data of Goose Bay may be affected by this phenomenon. Neither the Millstone Hill data nor the model dB values have taken into consideration the viewing geometry. As mentioned earlier, this will be part of Phase 2.

Appendix B

High Latitude Models and Averaged vs Median Data

In Figure B1 is shown the equation which results in the best-fitting model for Narssarssuaq and Goose Bay, for the latitude range 60° to 63°Λ. The 12 monthly plots, in local time, are shown in Figures B1a through B1l for the cases of low and high solar flux (80 and 140) under four selected magnetic conditions ($K_p = 0.5$, 2.5, 4.5 and 6.5). Under comparison with the individual station plots exhibited earlier, the major cause of inaccuracy in the fit is seen to be due to the erratic high K_p model in certain months, particularly at Goose Bay. This is possibly the result of insufficient data.

In order to substantiate the exclusion of Sagamore Hill data in the global model, an additional equation was produced (Figure B2) which results in the best-fitting model when data from all three stations were used. These equations are restricted to the latitude range 53° to 63°Λ. These monthly plots (Figures B2a through B2l) compare surprisingly well with those generated by the two-station model.

The actual data plotted in Figures 3, 5, and 10, upon which the model is based, are the averaged scintillation data in dB. It was desired to compare this mean with the calculated median for the same time, K_p, and solar flux blocks. Figures B3a B3b, and B3c illustrate both the mean and median dB values for Narssarssuaq, Goose Bay, and Sagamore Hill, respectively. This data is for the same time period (March) as described in the earlier figures. It can be seen that no substantial differences occur between the averaged and median dB values at any of the stations, except that as discussed under the topic of distribution of SI readings, for low scintillation activity averaged values tend to be higher than median values.

29

I. Narssarssuaq — Goose Bay based.

$$SI = -1.3 - 2.7\,CL + 6.2(1 - .17(1 + 2.6\,CL)\,FD)\left[1 + .33(1 - .35(1 - .8\,CL)\,FD)\cos(HL + 2.1 - 4\,Kp)\right.$$

$$\left. + .05\cos(2(HL - .9)) + .02\cos(3(HL + 3.5))\right](1 - .9\,CL)\ EXA$$

$$\text{where } EXA = 2\left[.2\,Kp(1 + .13\,FD) + .75\,As\,CL(1 + FD)\right]$$

$$As = S_f/100$$

$$HL = \text{local time (hr.)}$$

$$FD = \cos(DA - 2.6) + .2\cos(2(DA - 30))$$

$$PF = \text{Geomag. Lat. (deg.)}$$

$$CL = \cos((PF - 53.5)\,\pi/25)$$

$$\left[\dfrac{2\pi}{365} \ \& \ \dfrac{2\pi}{24} \text{ implied in all annual } \& \text{ diurnal periodic terms}\right]$$

(see text)

Figure B1. Mathematical Model of Scintillation Based
Upon Narssarssuaq and Goose Bay Data

Legends for data shown in Figures B1a through B1l and B2a through B2l:

| B1a through B1l	B2a through B2l
————— - Narssarssuaq	—————— Narssarssuaq
—————— Goose Bay	————— Goose Bay
	———————— Sagamore Hill
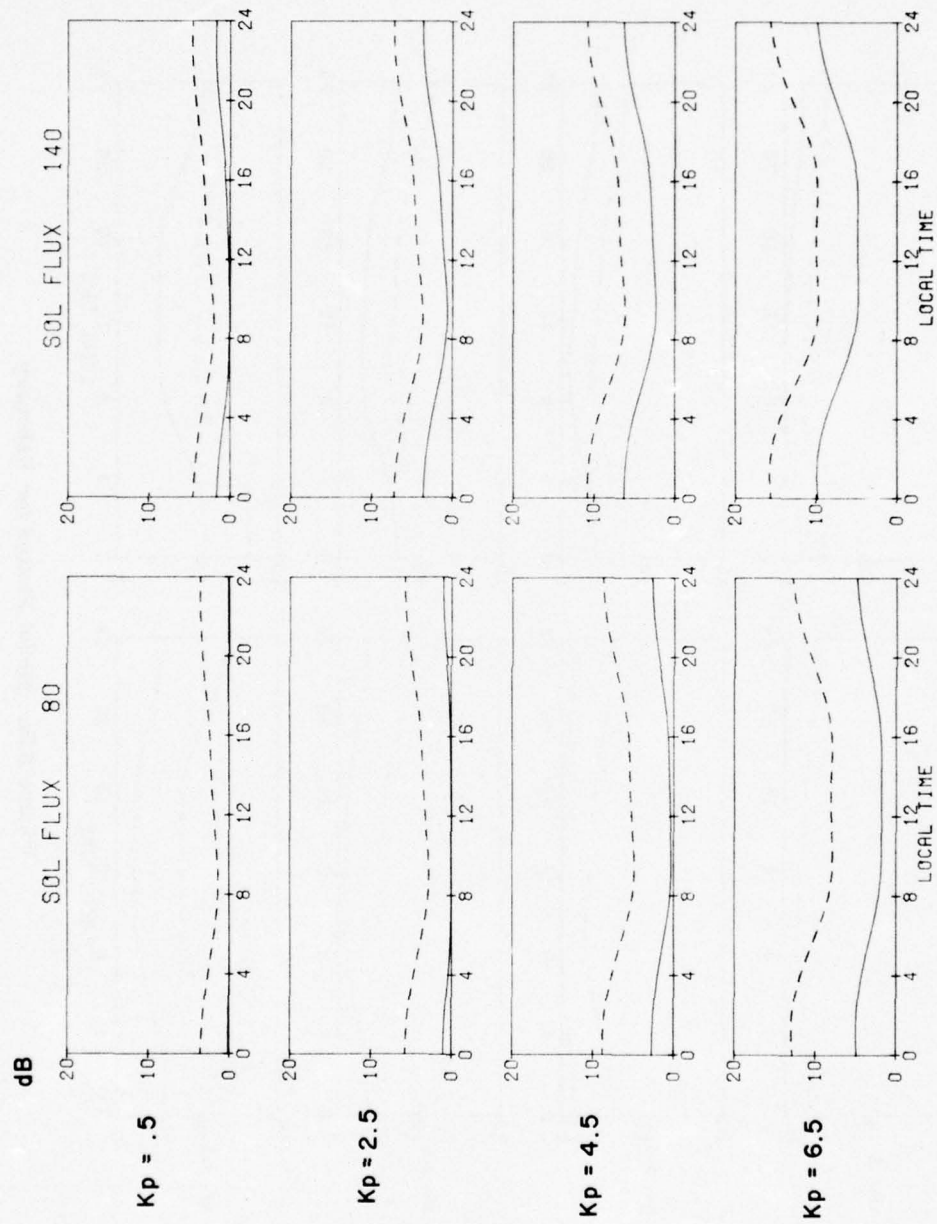
Figure B1a. Model Plotted for January

31
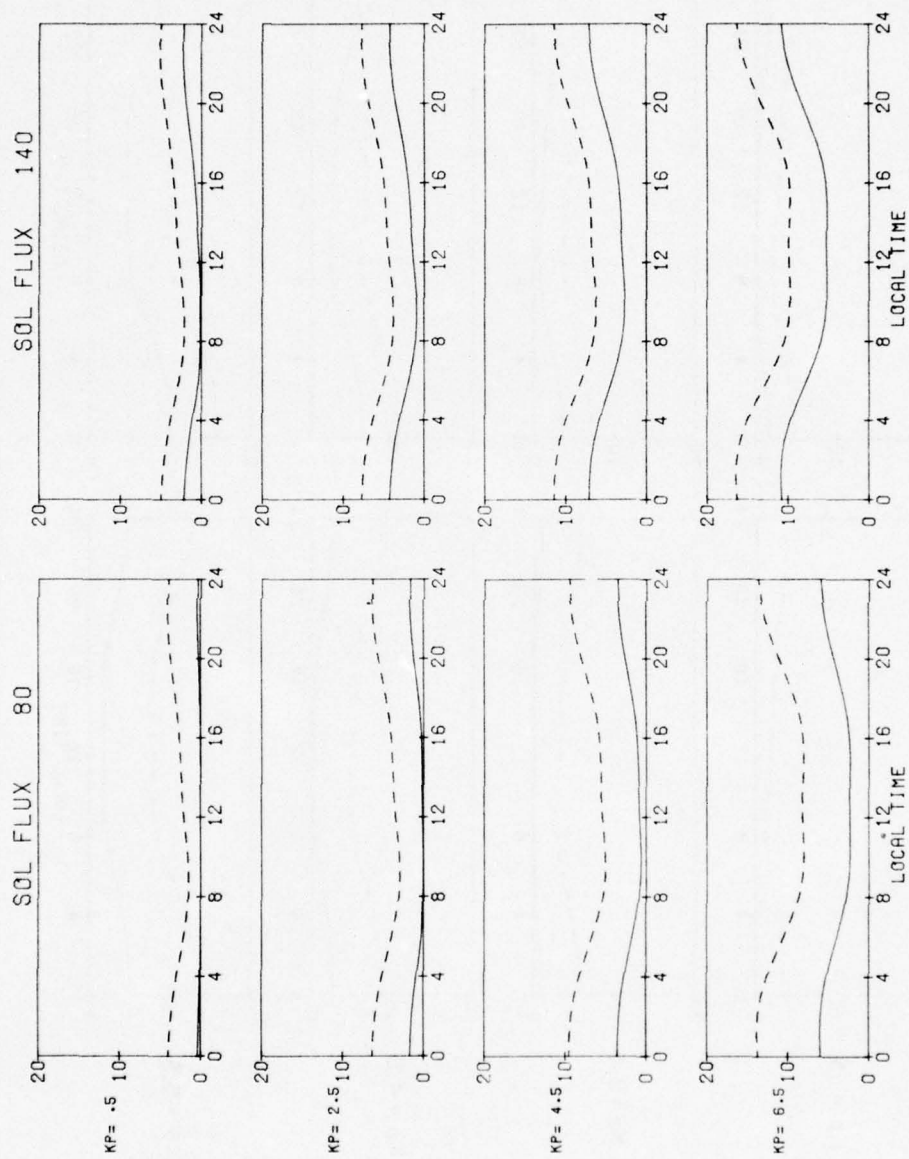
Figure B1b. Model Plotted for February

32
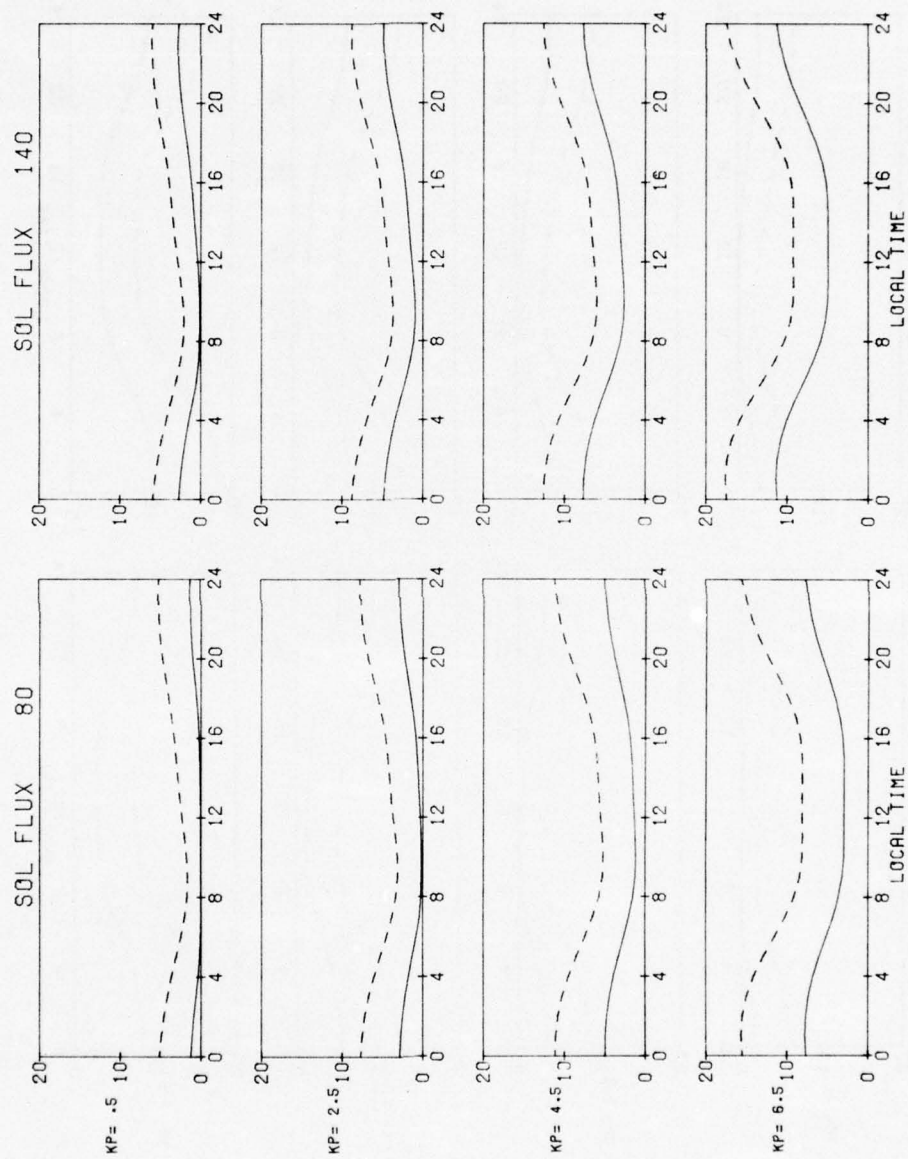
Figure B1c. Model Plotted for March
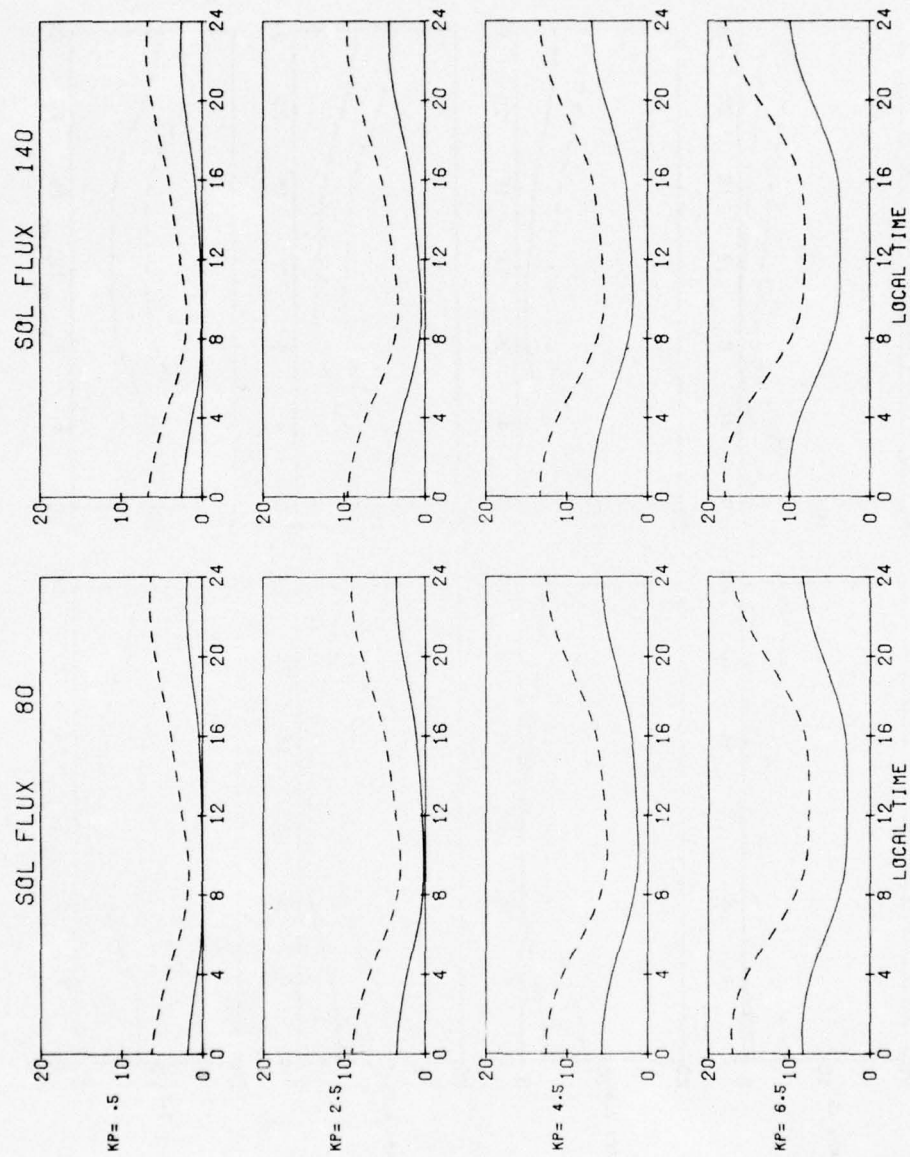
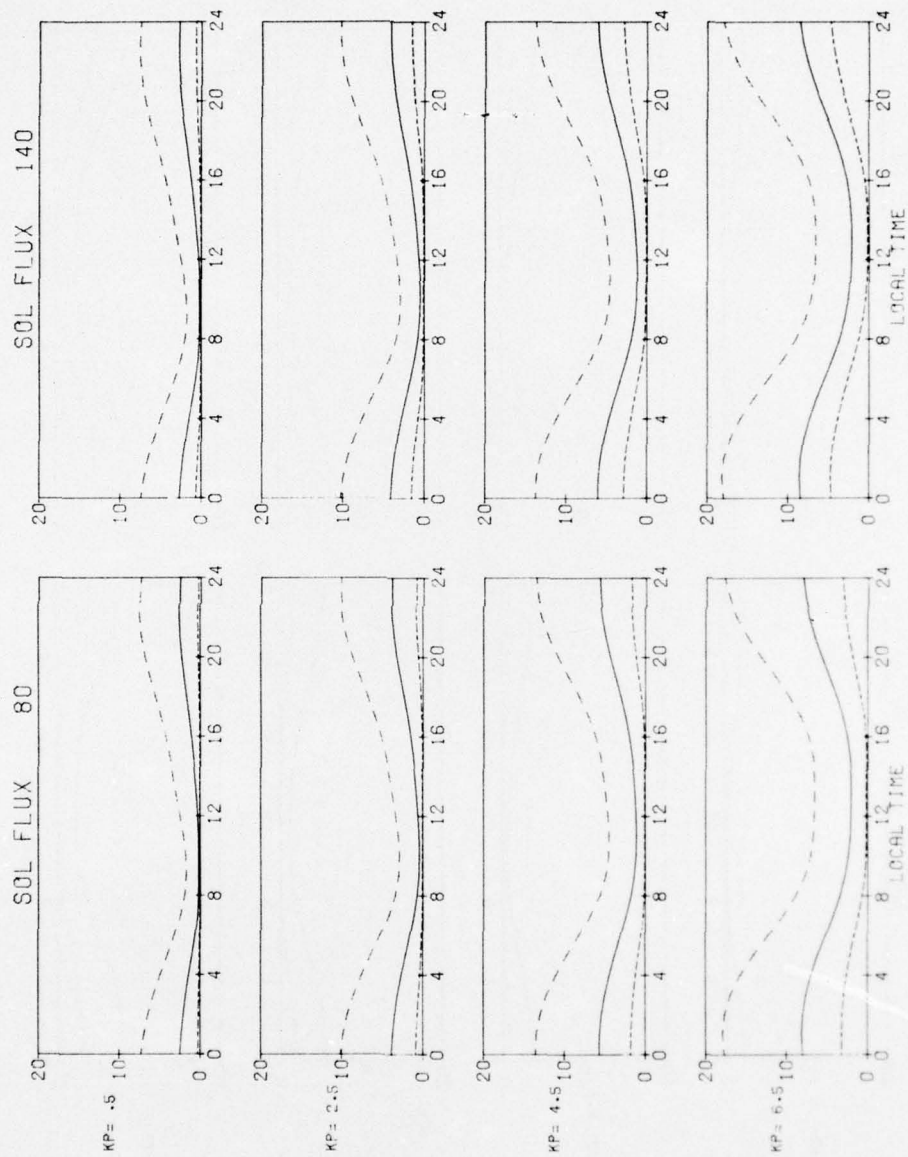Figure B1d. Model Plotted for April

34
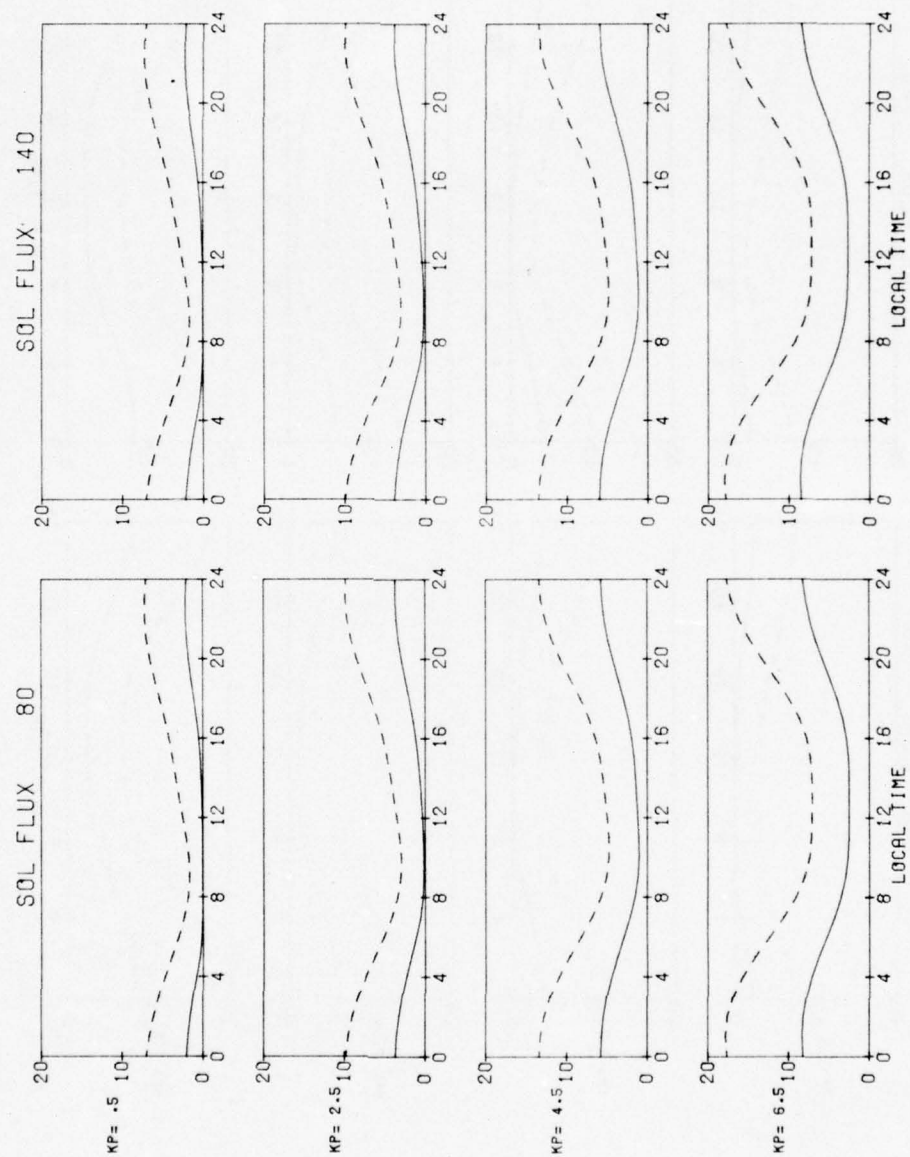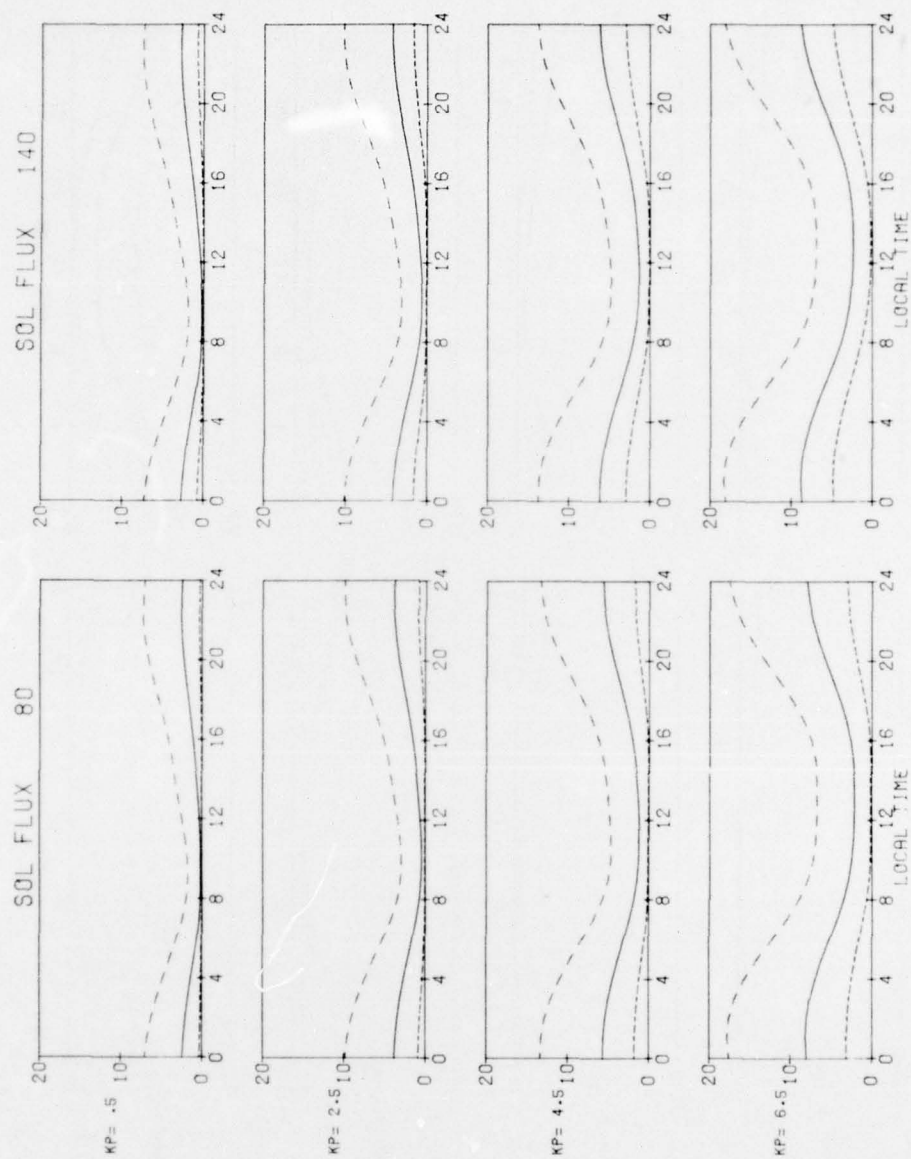
Figure B1e. Model Plotted for May
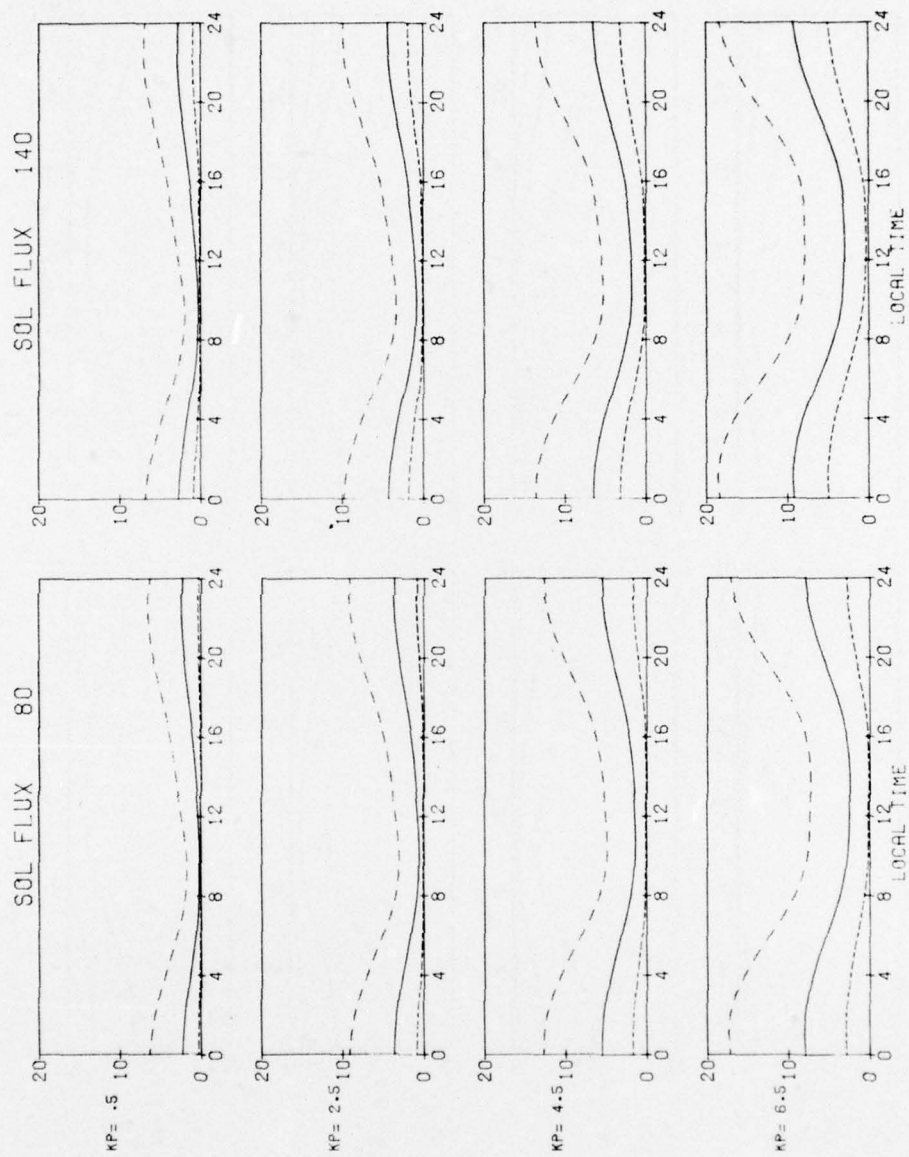
35
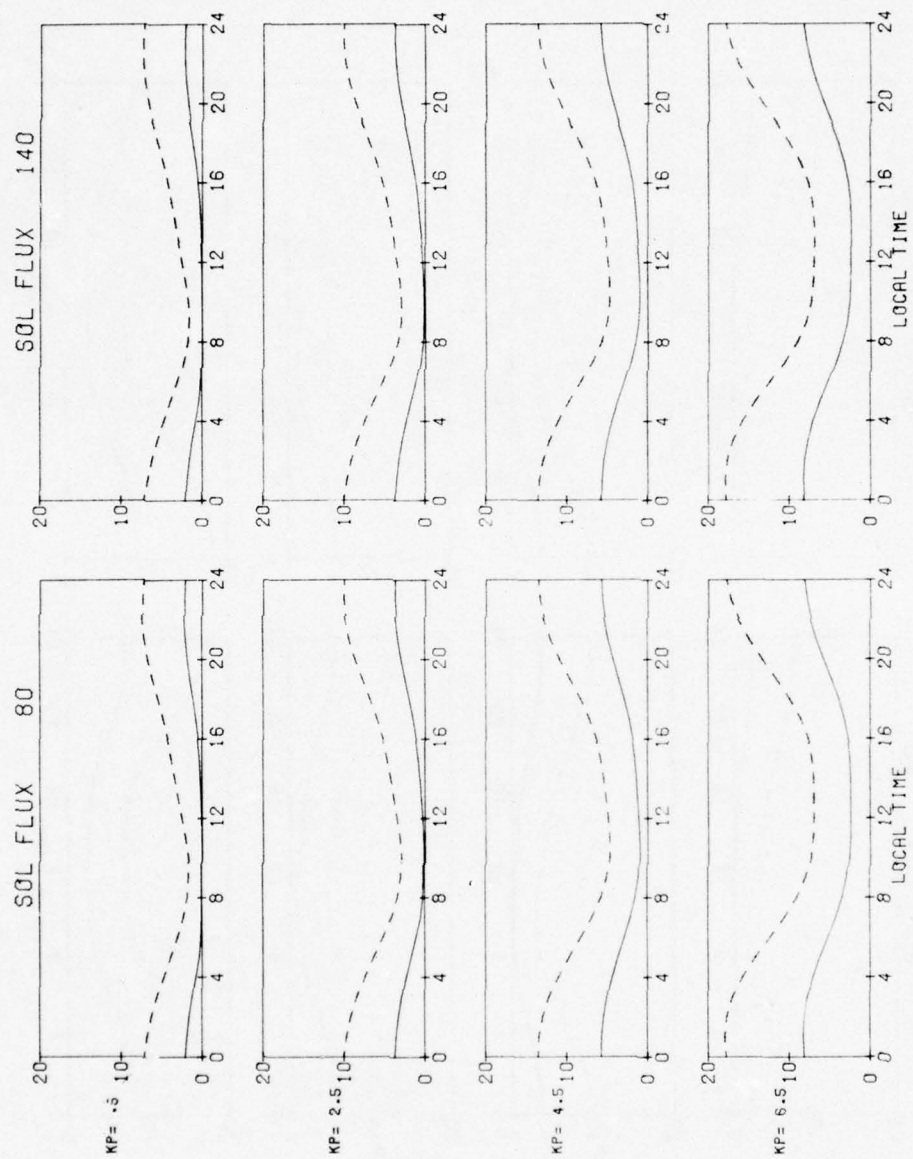
Figure B1f. Model Plotted for June

36
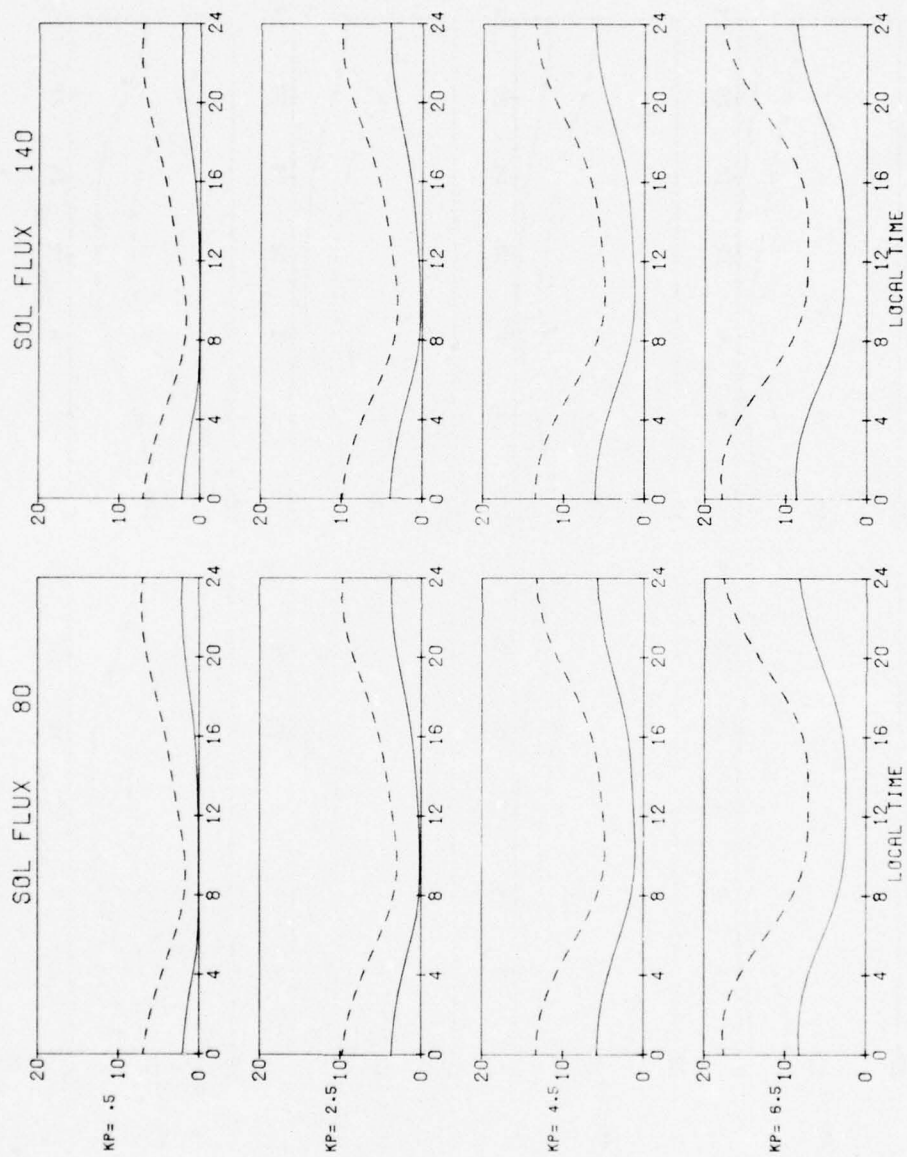
Figure B1g. Model Plotted for July

37
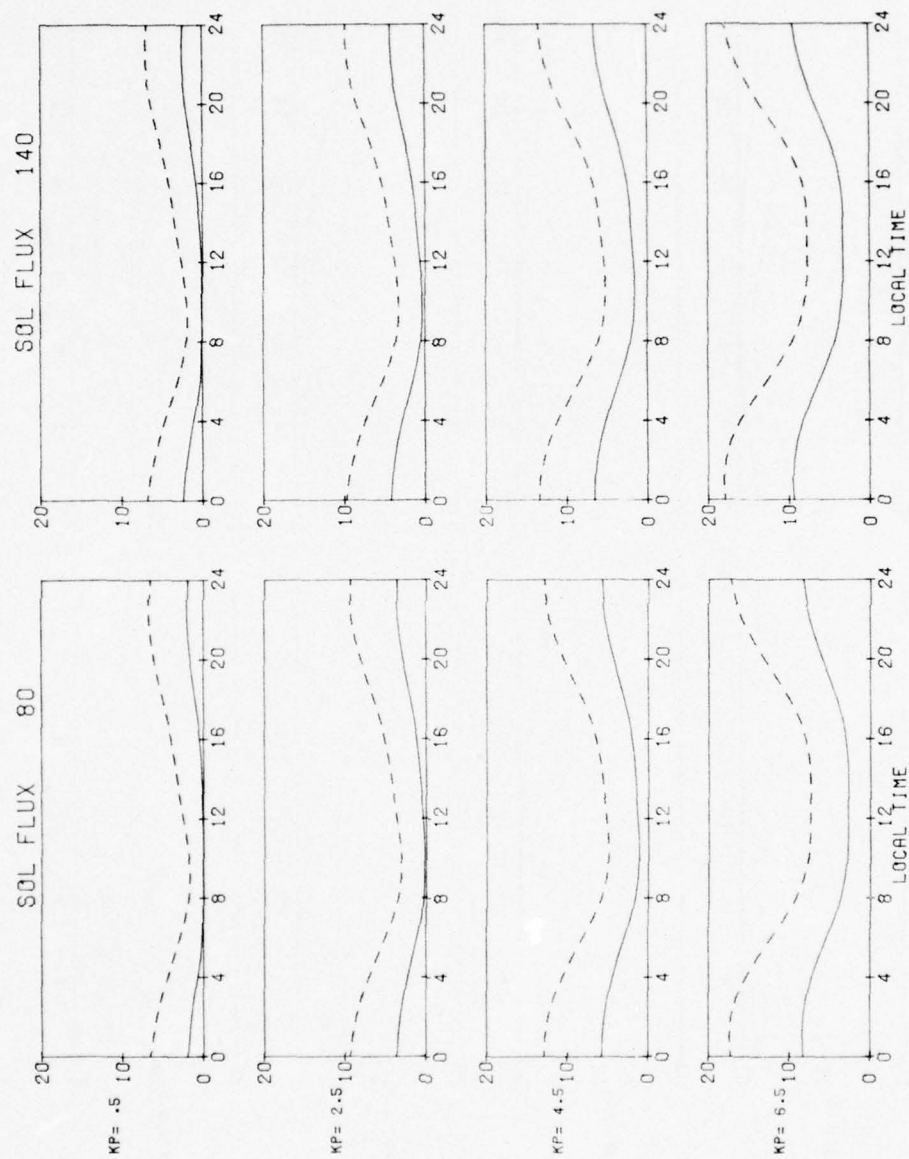
Figure B1h. Model Plotted for August

38
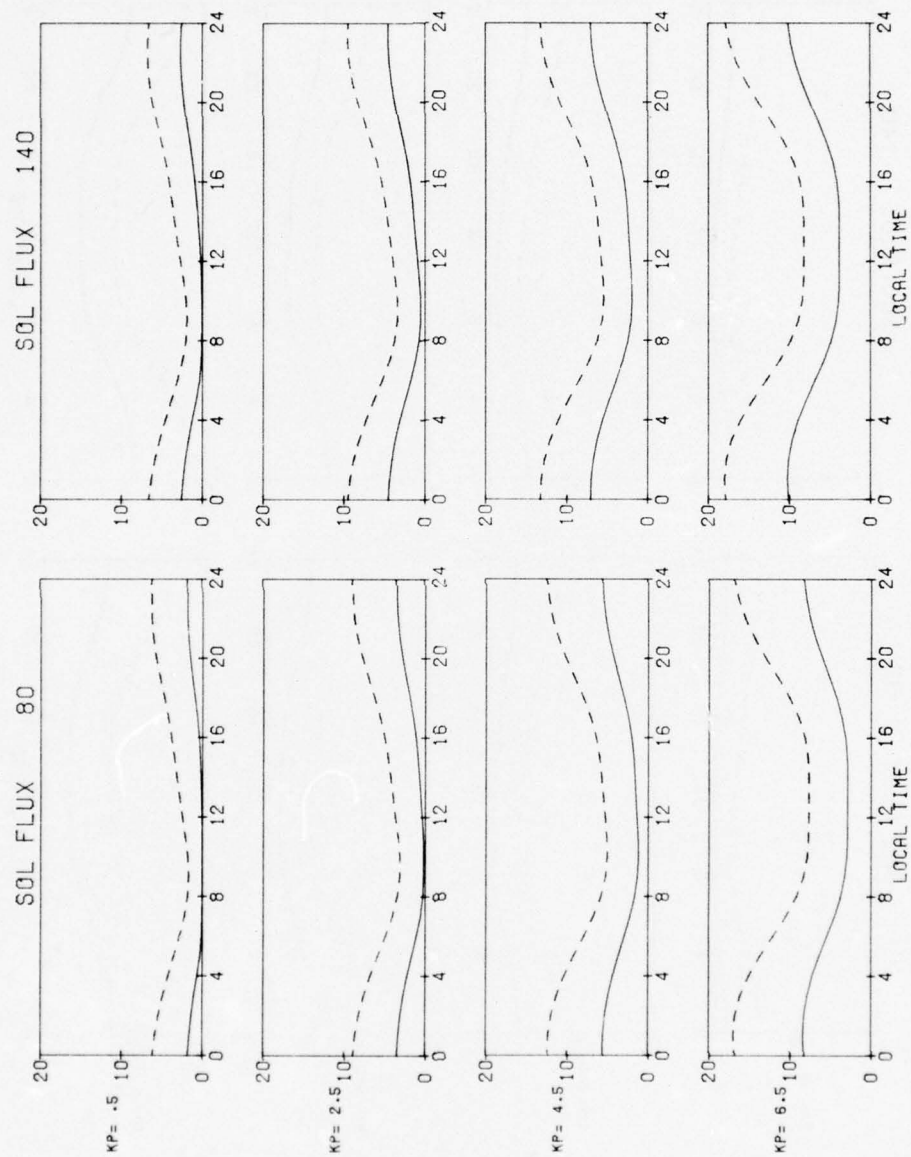
Figure B1i. Model Plotted for September
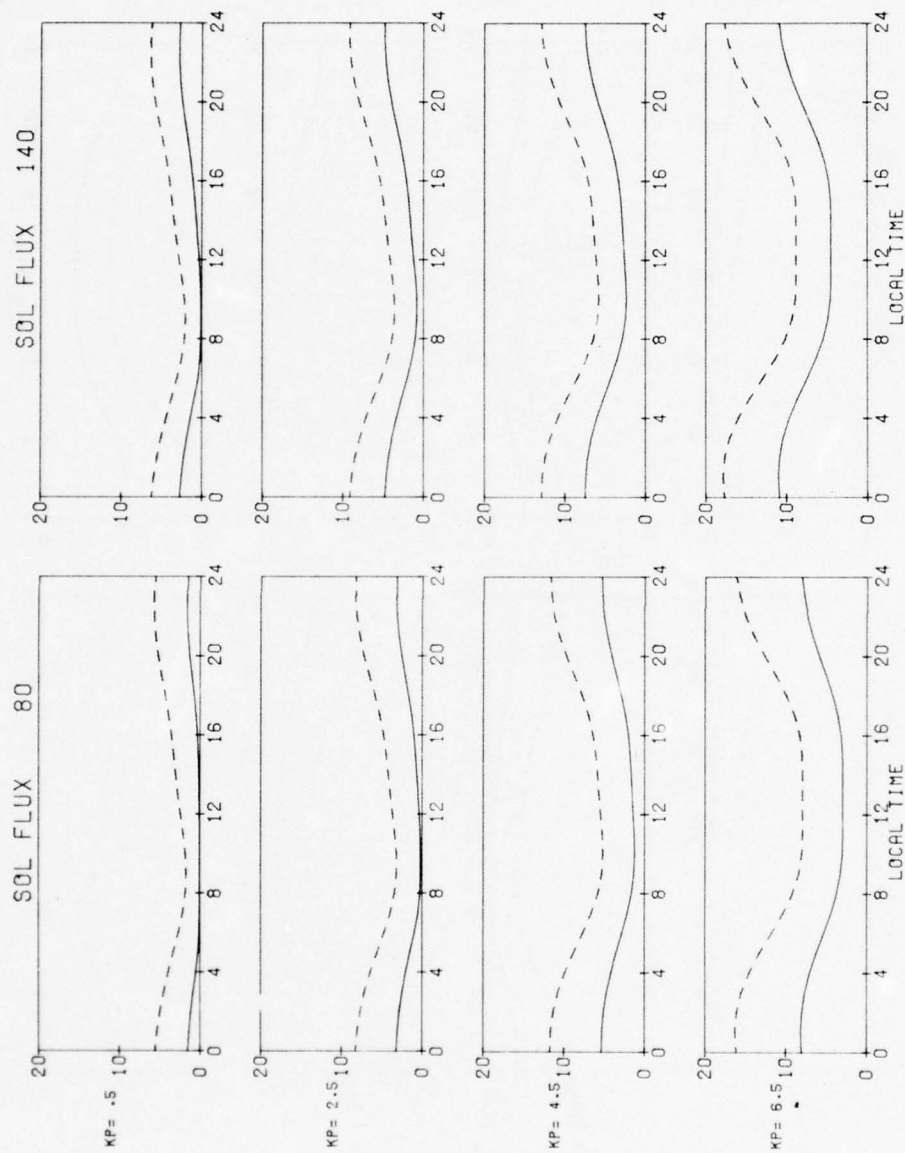
Figure B1j. Model Plotted for October

40
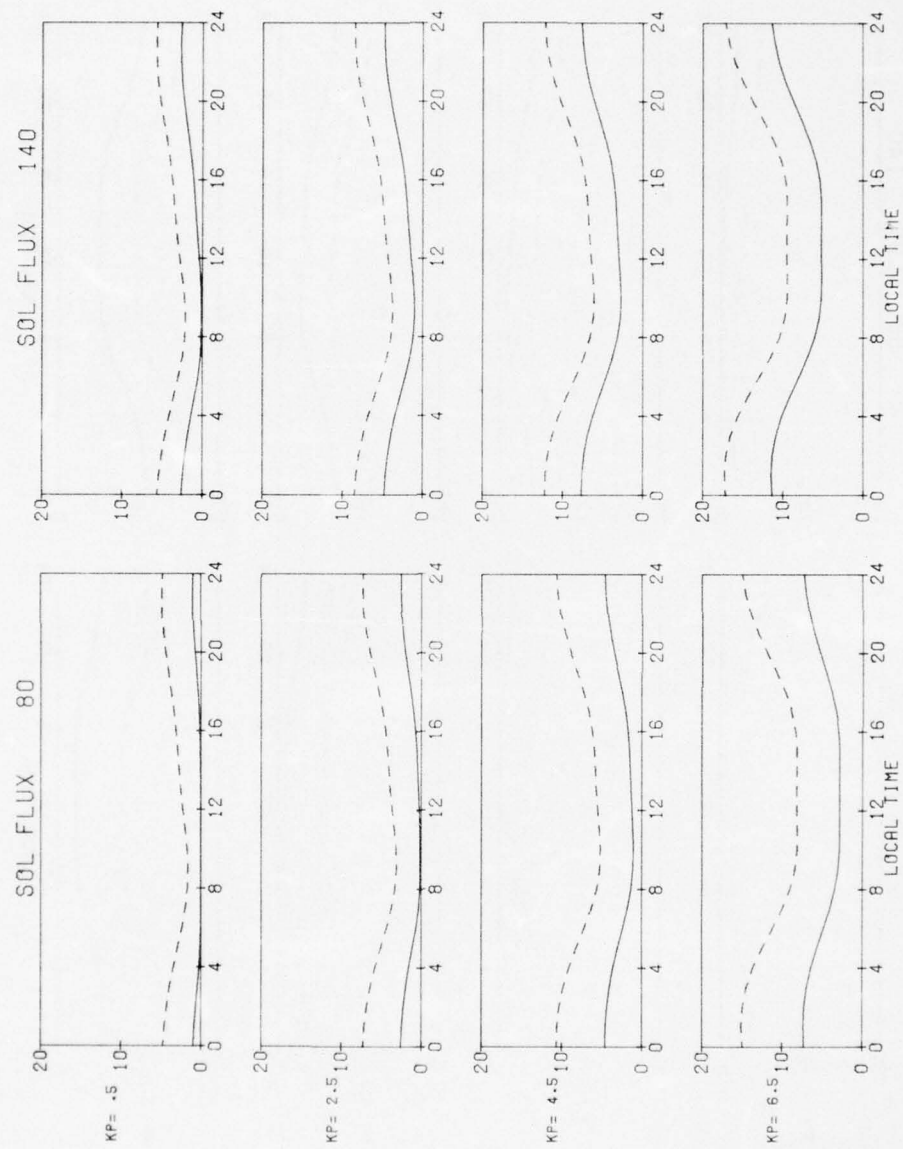
Figure B1k. Model Plotted for November

41
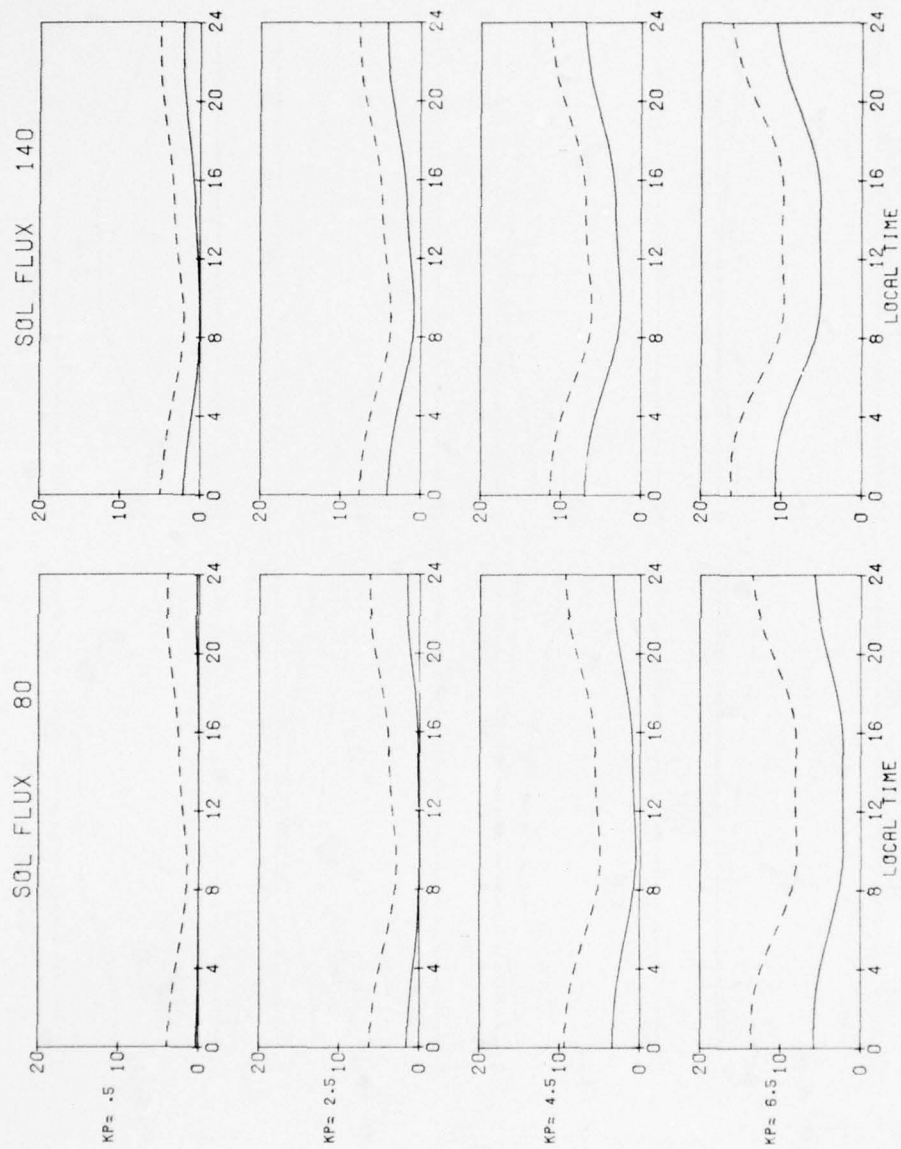
Figure B11. Model Plotted for December

42

II. Narssarssuaq — Goose Bay — Sagamore Hill based.

$$SI = -2.0 + 1.2\,CL + 6.5\,(1 - .2\,FD)\Big[1 + .6\,(1 - .16\,FD)(1 - .5\,SL)\cos(HL + 2 - .4\,Kp)$$

$$+ .05\cos(2(HL - .9)) + .02\cos(3(HL + 3.5))\Big]\,(1 - CL)\,EXA$$

$$\text{where } EXA = 2^{\big[.2\,Kp(1 + .2\,CL)(1 - .1\,XD) + As(1 - .8\,SL)(1 + .45\,FD)\big]}$$

where $\begin{cases} CL = \cos((PF - 54.4)\,\pi/25) & CDL = 1 + .7\,SL \\ SL = \sin((PF - 54.4)\,\pi/25) & SDL = 1 - .3\,SL \end{cases}$

$$PD = \cos(DA + 16) + .3\cos(2(DA - 30))\,; \quad FD = CDL \times PD \quad XD = SDL \times PD$$

Figure B2. Mathematical Model of Scintillation Based Upon Narssarssuaq, Goose Bay, and Sagamore Hill Data

43
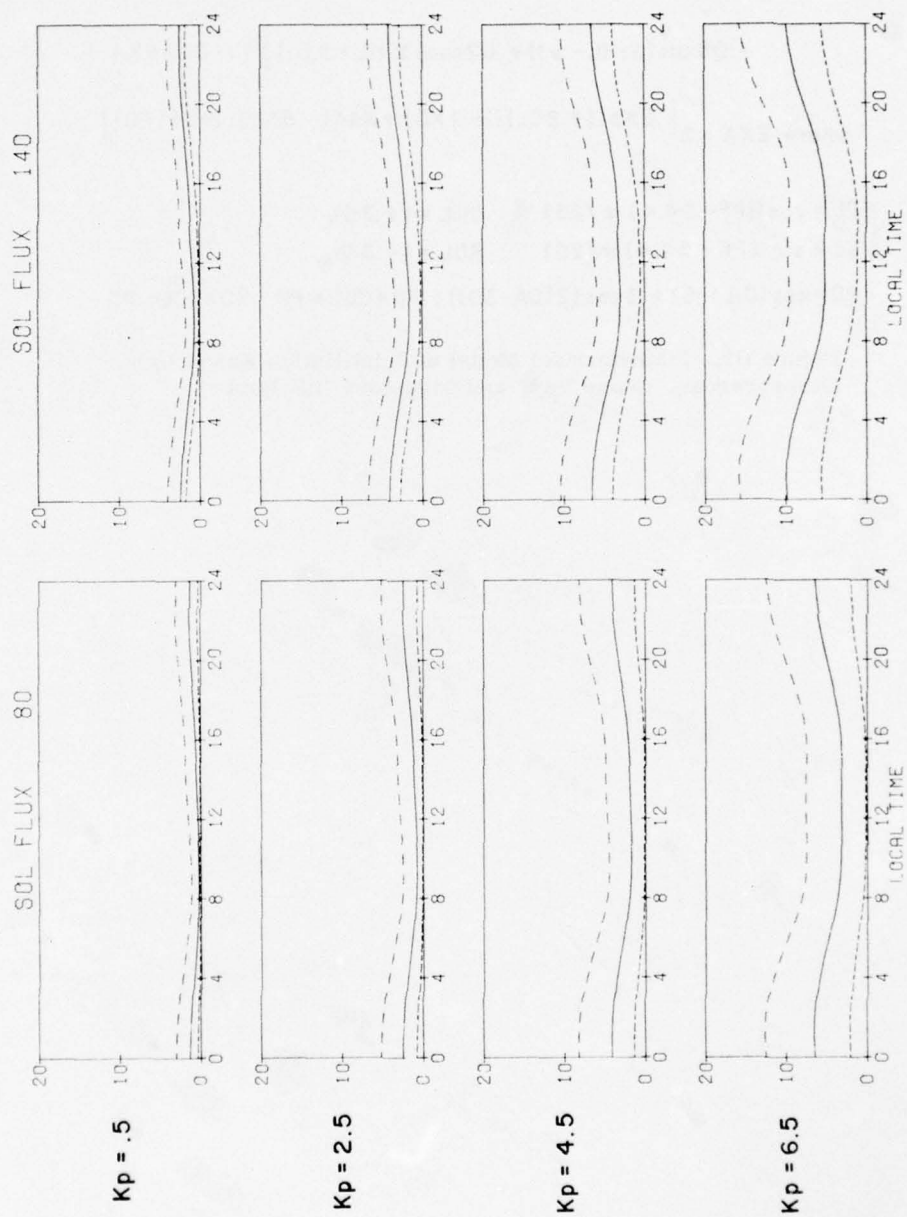
Figure B2a. Model Plotted for January

44
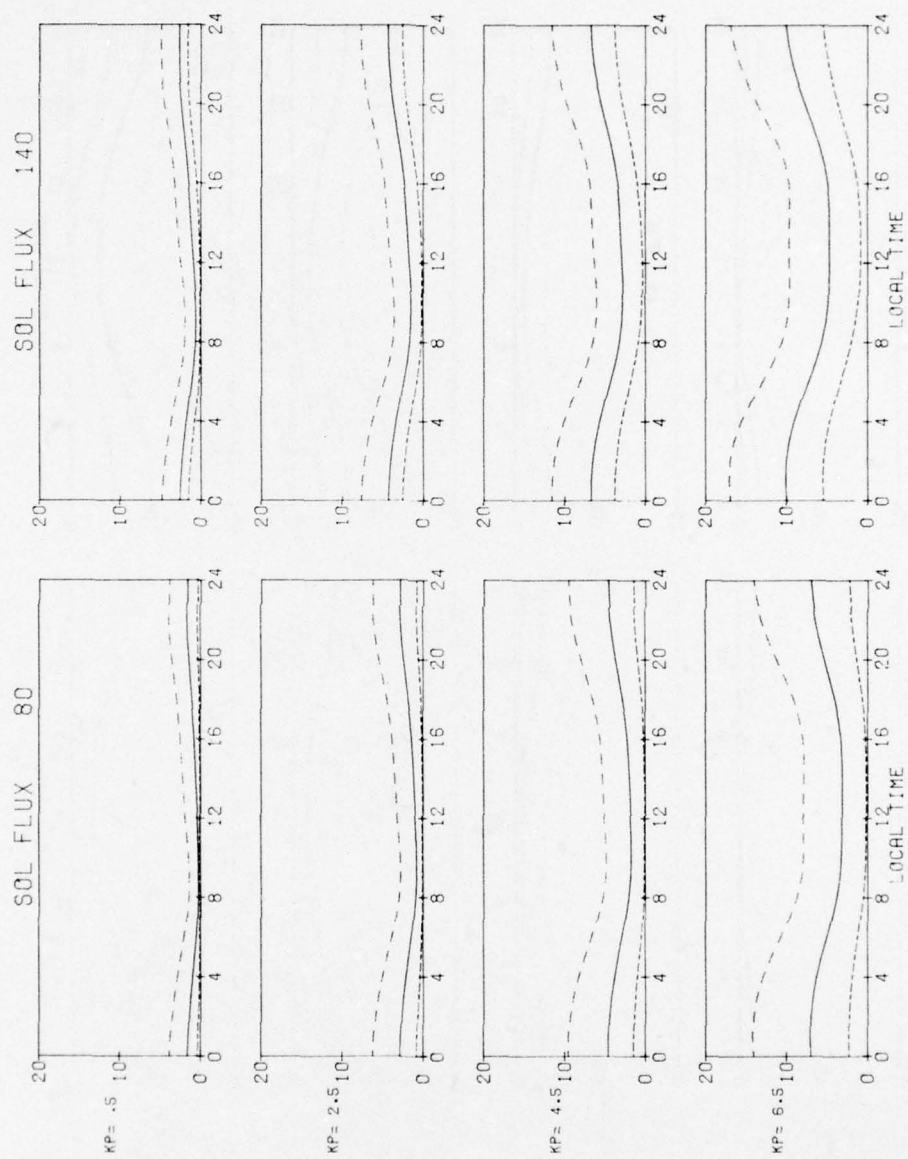
Figure B2b. Model Plotted for February
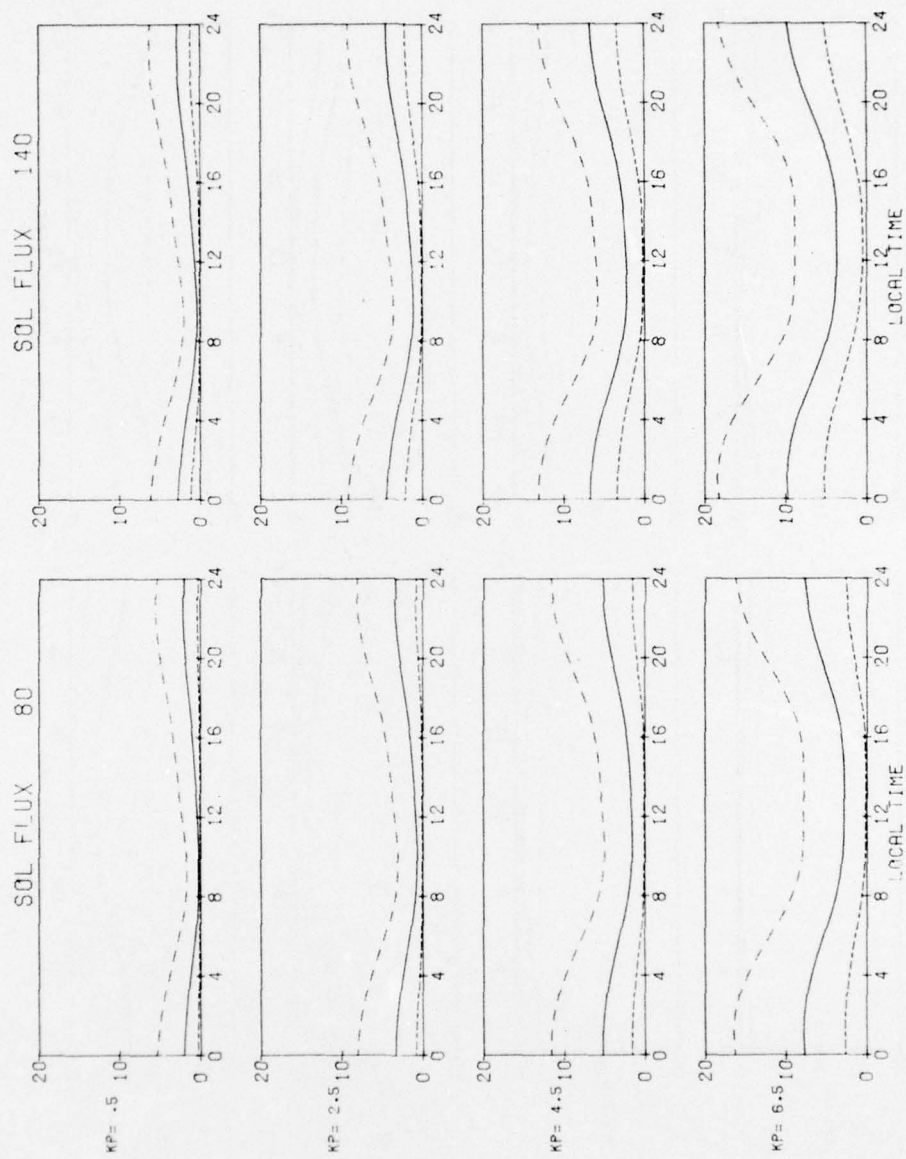
Figure B2c. Model Plotted for March

46
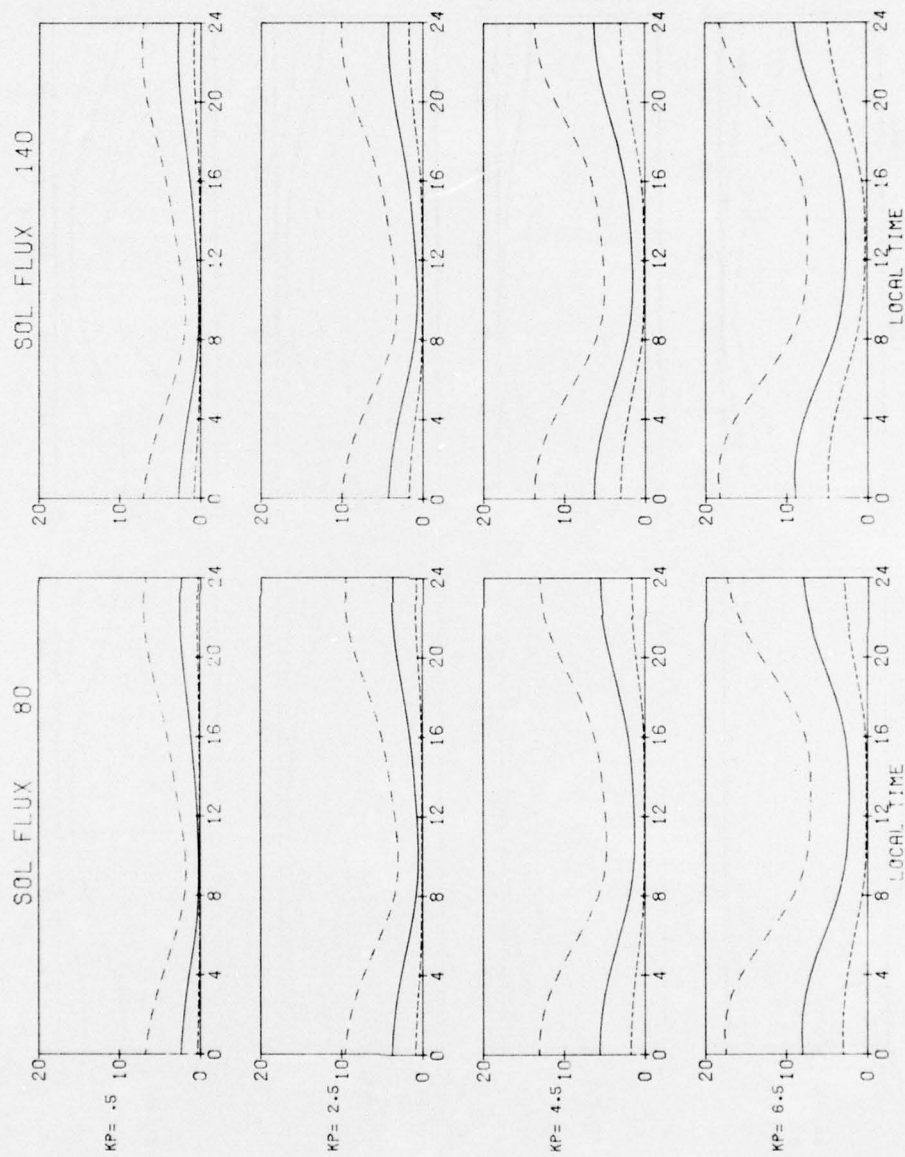
Figure B2d. Model Plotted for April

47

Figure B2e. Model Plotted for May

48

Figure B2f. Model Plotted for June

49

Figure B2g. Model Plotted for July
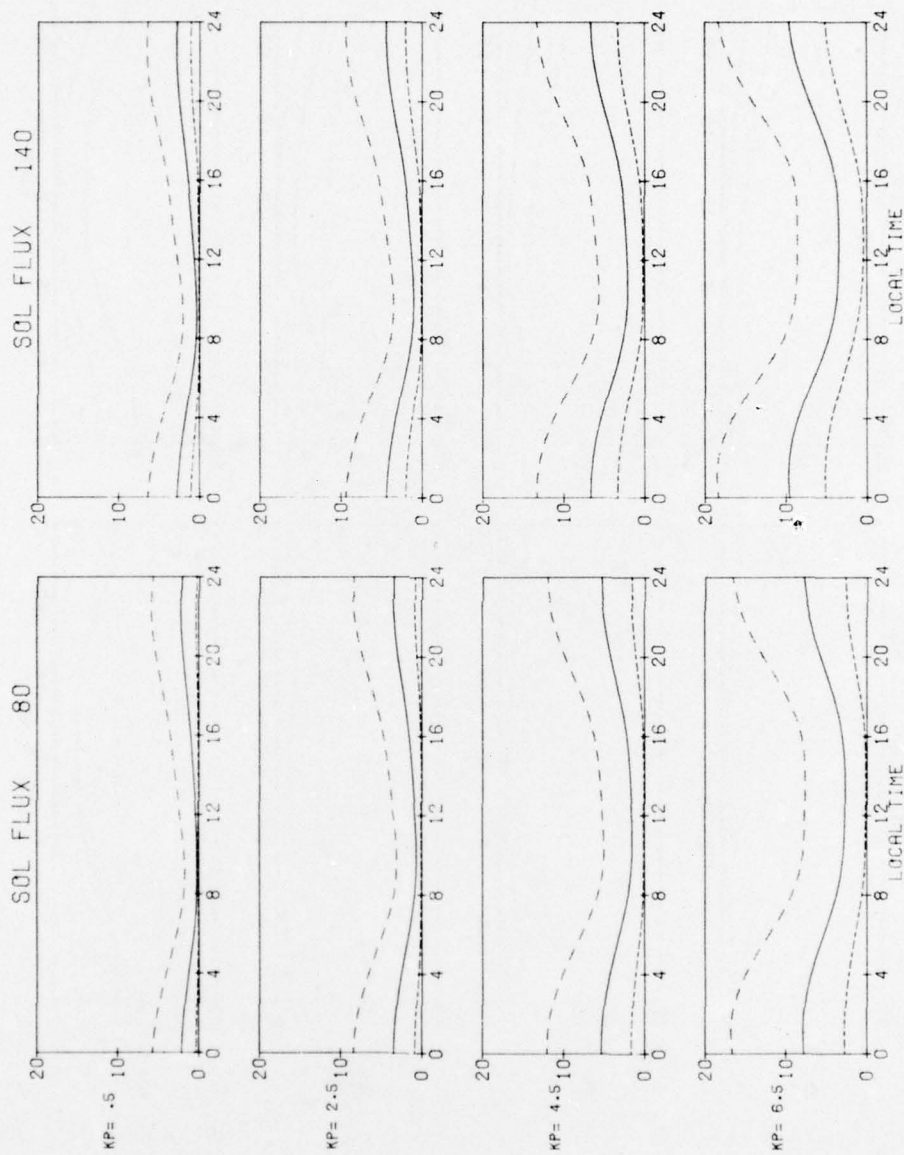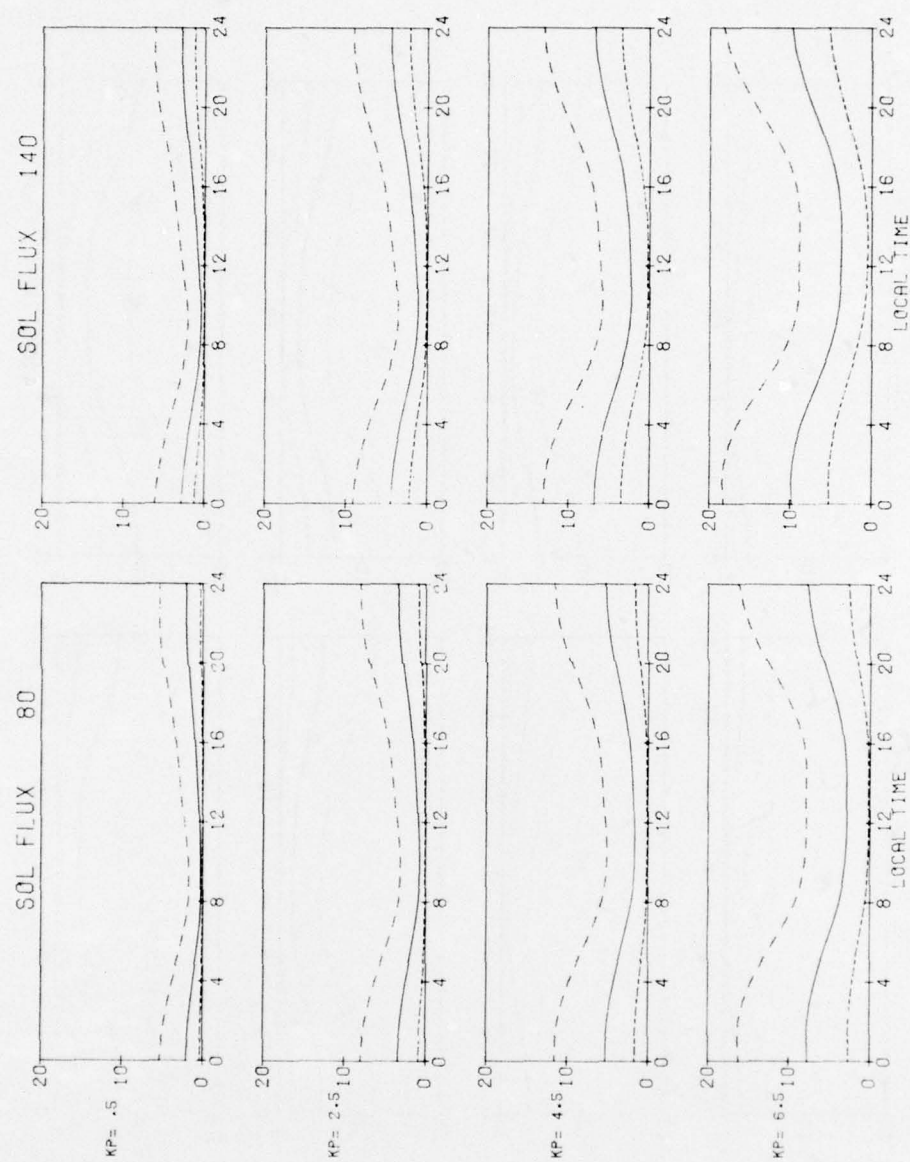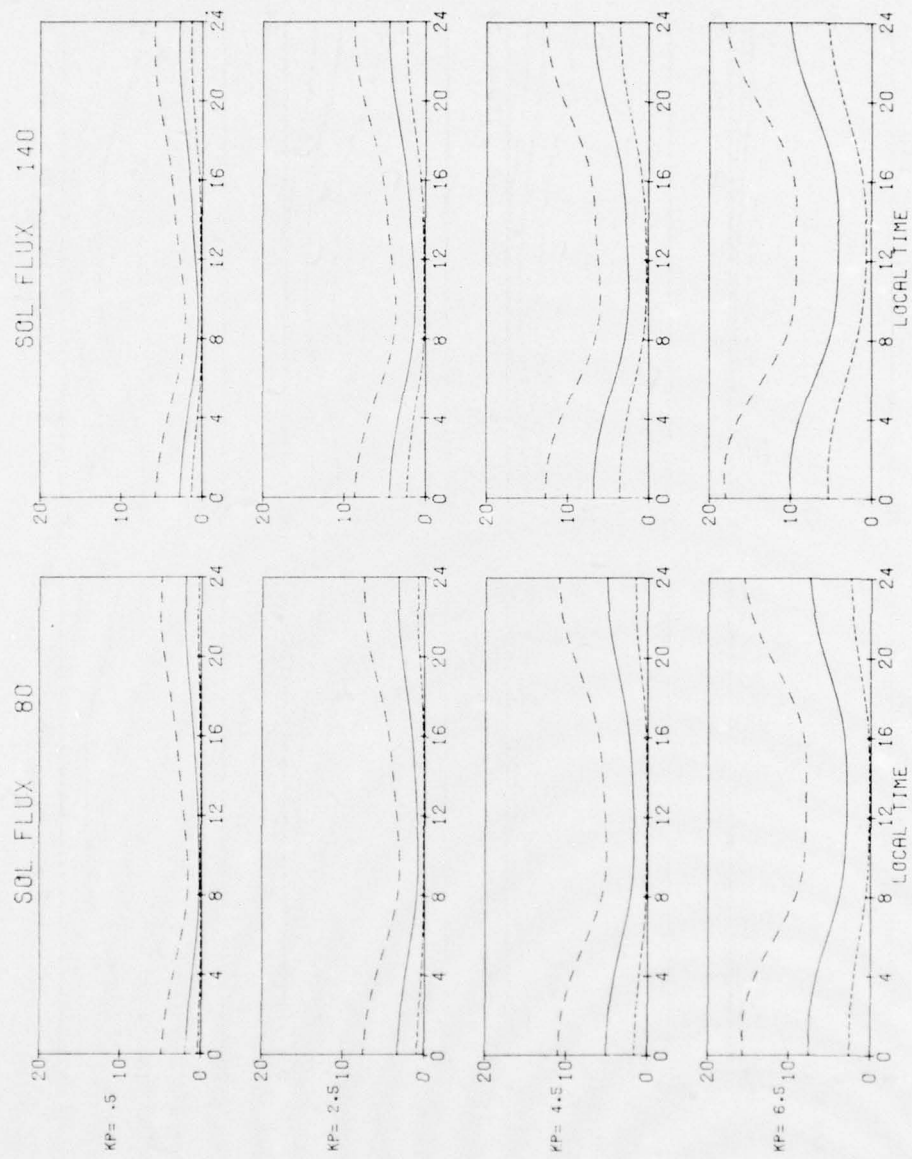
Figure B2h. Model Plotted for August

51

Figure B2i. Model Plotted for September

52

Figure B2j. Model Plotted for October
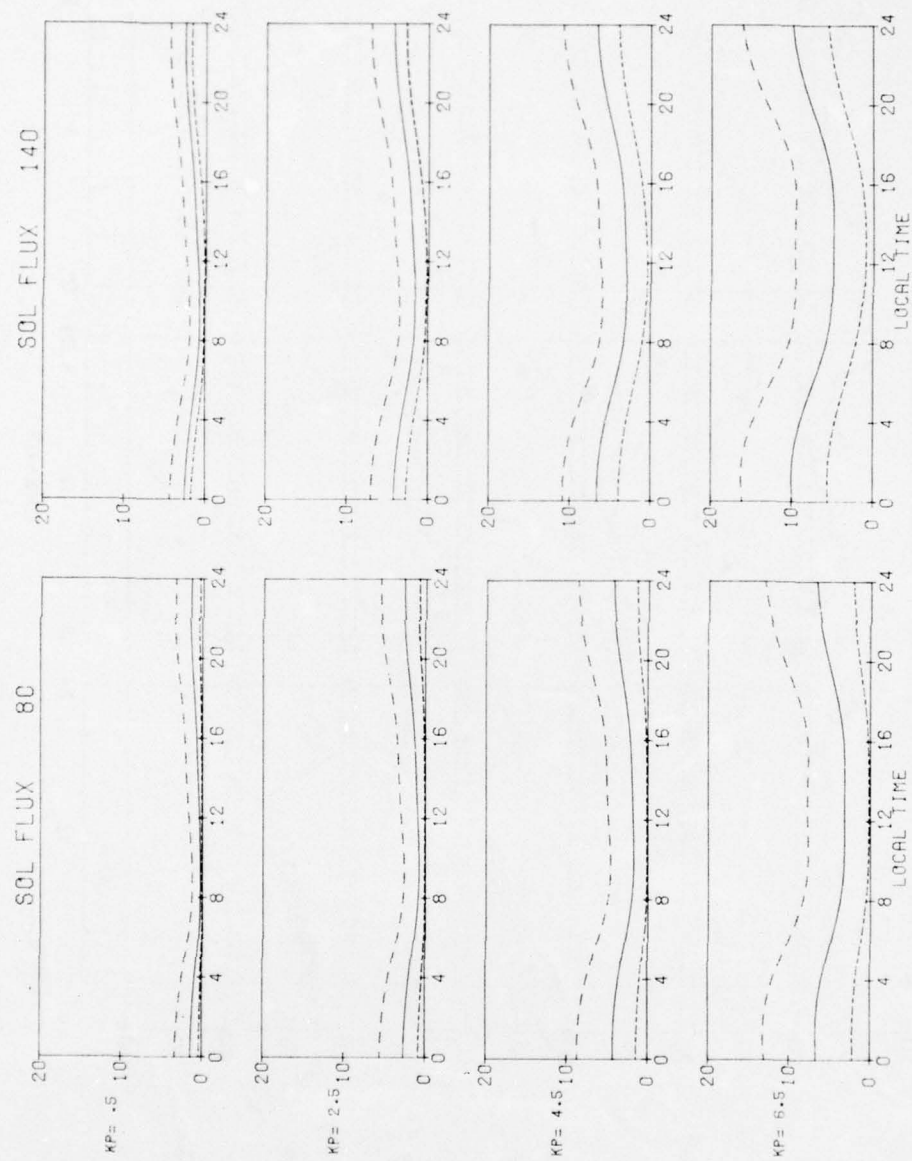
53
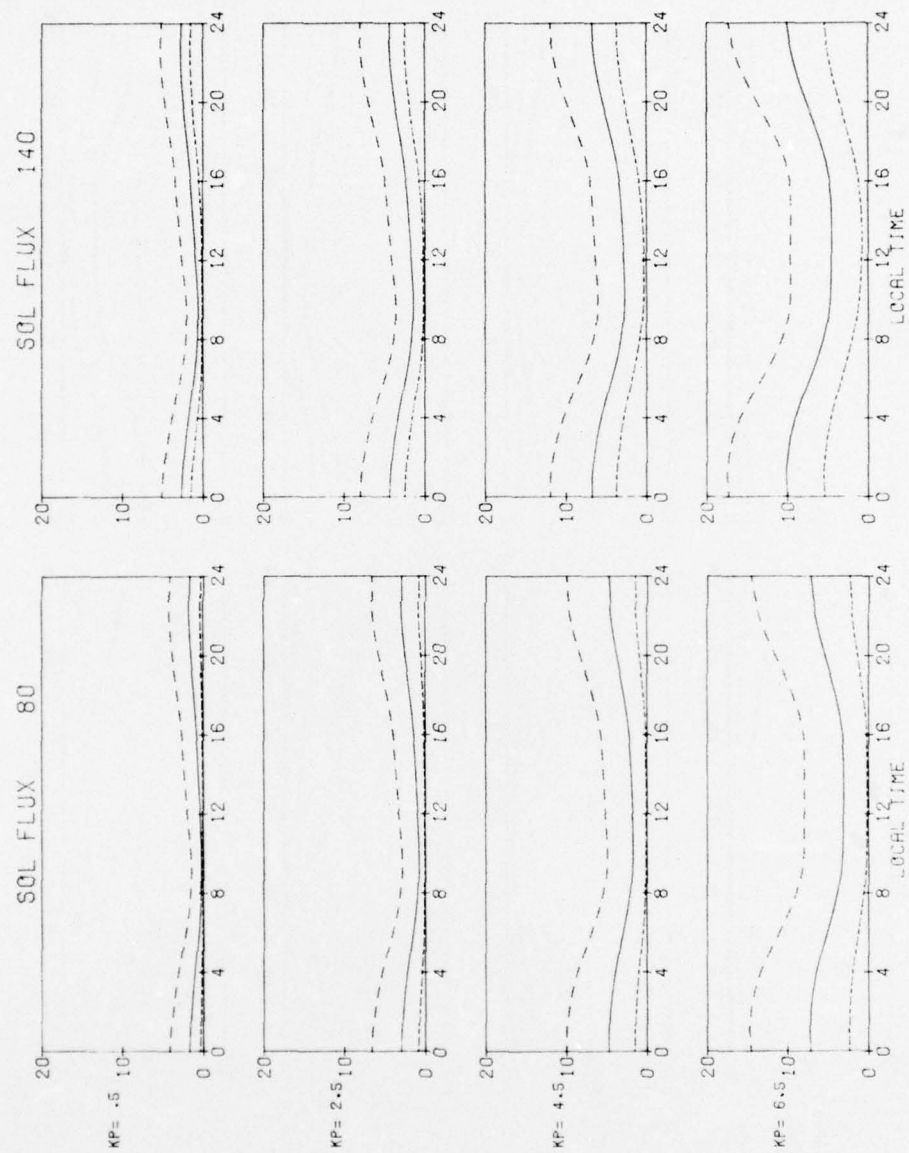
Figure B2k. Model Plotted for November
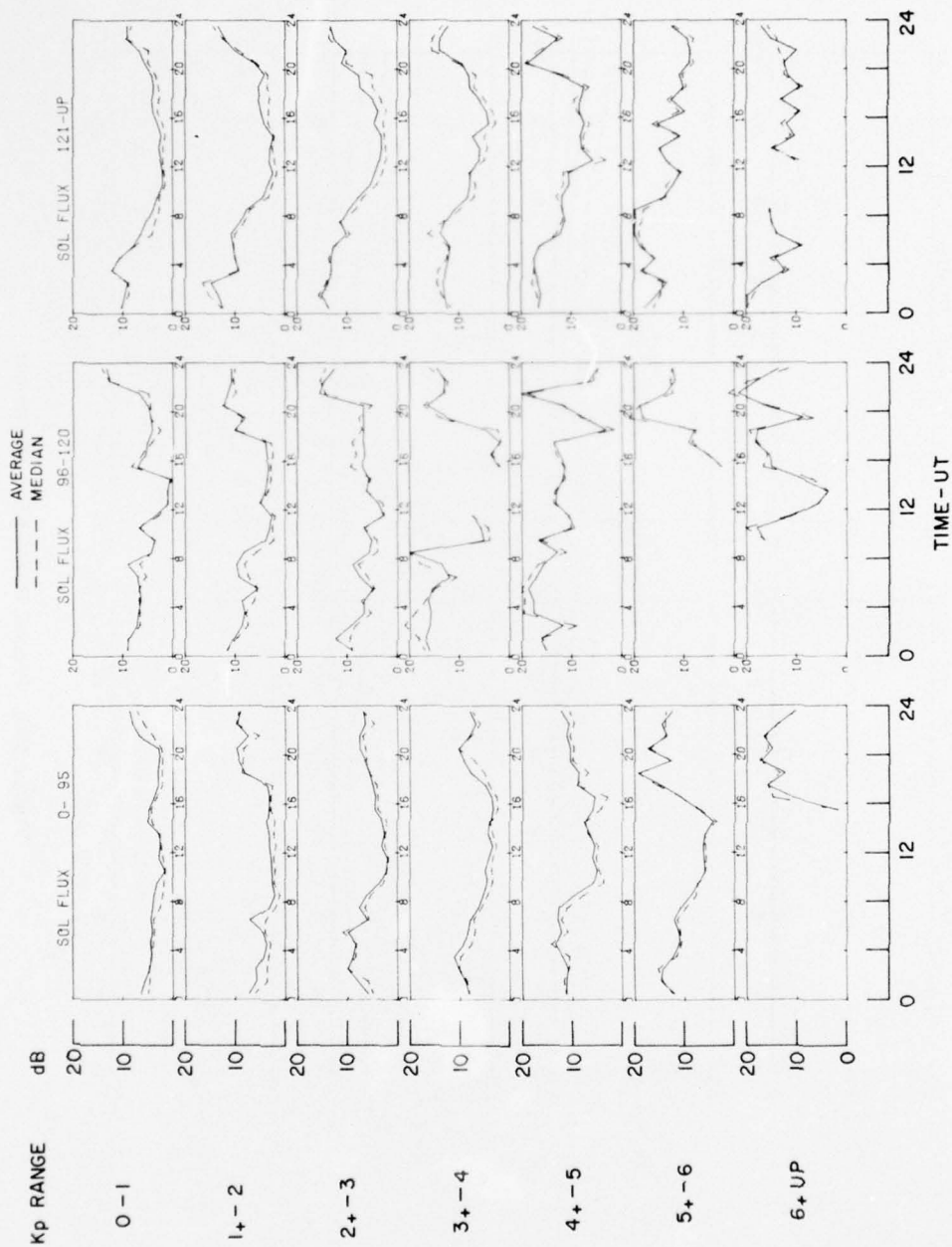
54

Figure B21. Model Plotted for December

55

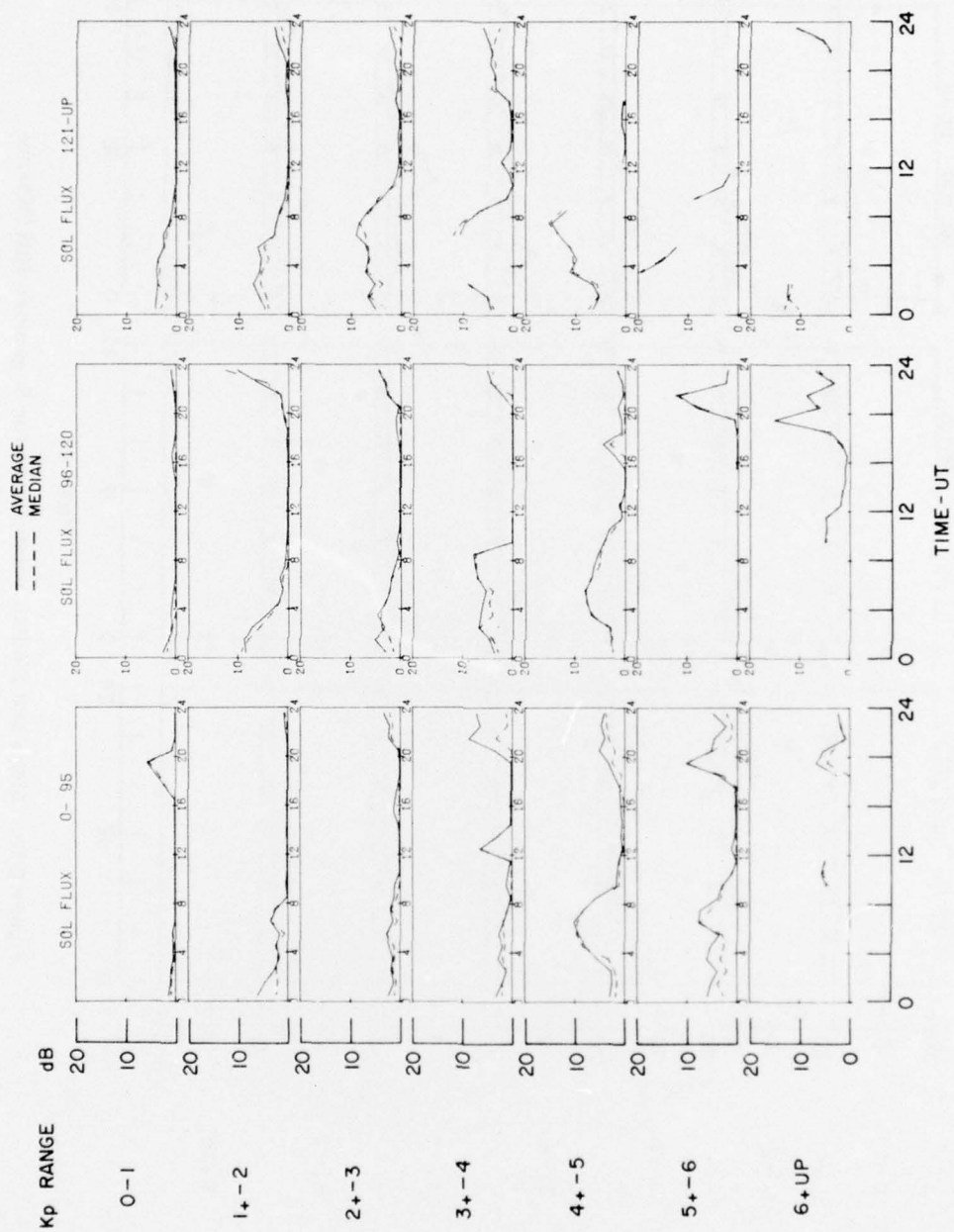Figure B3a. Mean and Median Scintillation for Narssarssuaq (March)

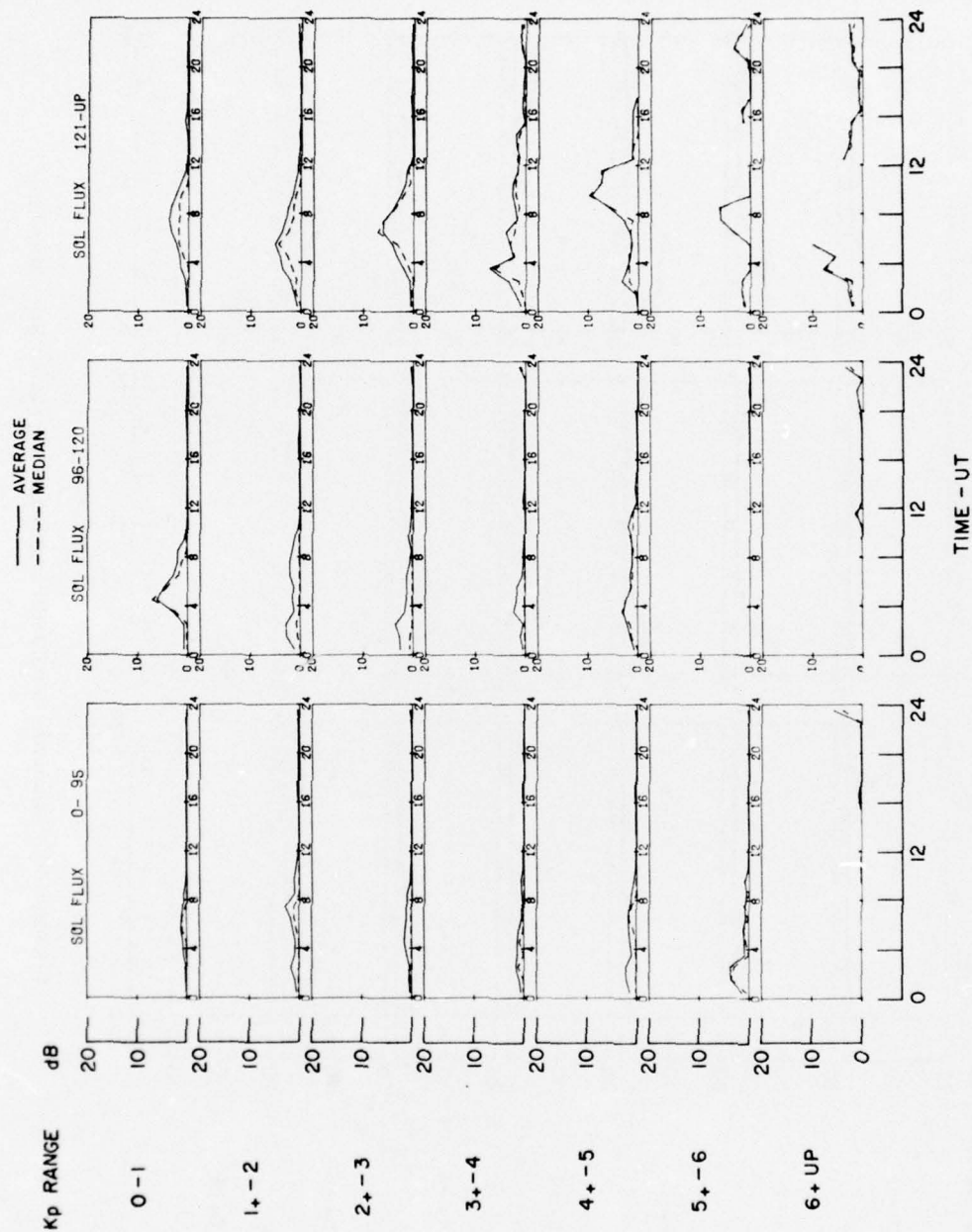Figure B3b.   Mean and Median Scintillation for Goose Bay (March)

Figure B3c. Mean and Median Scintillation for Sagamore Hill (March)